Western Australia School of Mines
Minerals, Energy and Chemical Engineering

Drilling Mechanics Group

A Method to Derive Rock Strength from the Drilling Response of Impregnated Diamond Bit

Hing Hao Chan

0000-0002-0912-2464

This thesis is presented for the Degree of
Master of Philosophy
of
Curtin University

January 2022

To the best of my knowledge and belief this thesis contains no material previously published by any other person except where due acknowledgement has been made. This thesis contains no material which has been accepted for the award of any other degree or diploma in any university.

Hing Hao Chan

12 January 2022

Acknowledgements

This study will not be completed without the assistance and support of a group of people. First and foremost, I would like to express my gratitude to my supervisor, Dr Masood Mostofi for his confidence in me and for allowing me to participate in academic research. His concern, inspiration, and encouragement broadened my views and provided me with new perspectives.

I would want to thank my associate supervisor, Dr Thomas Richard, for his assistance. He always keeps an eye on the research's progress and points out the research's derived themes, which keeps me motivated to finish the project.

I'd also like to express my gratitude to the Mineral Exploration (MinEx CRC) for providing me with financial aid.

Without Rui Huang's help, who was constantly present during my experiment, my research would not have been possible. Most importantly, his willingness to take the initiative to make procurement has relieved me of any additional concerns as I conduct my investigation.

In addition, I'd want to express my gratitude to my parents for their sound advice and sympathetic ear. They are always willing to help me out. Finally, I couldn't have finished this dissertation without the help of my friends, Ethan Tong, Vhui Tao Chang, Henry Lee, De Kern Yap and Jun Wei Wong, who provided intriguing talks as well as cheerful distractions to take my mind off my study.

Abstract

The mining and petroleum industries use impregnated diamond bits for hard rock drilling and coring. Several drilling response models have been proposed to understand impregnated diamond bit's drilling response, however, the validations of those models were mostly done with little rock collection, and mainly on sedimentary rocks. This study aims to create a drilling methodology for impregnated diamond bit on abrasive rocks in a laboratory scale. A kinematically controlled laboratory scaled drilling rig named Echidna controls feed rate and angular velocity. At the same time, the rig possesses sensors that measure weight-on-bit and torque-on-bit at high precision. The study determines intrinsic specific energy under the Franca-Mostofi model framework at various rock collections, including highly abrasive crystalline rocks. The experimental result suggests a robust linear relationship between intrinsic specific energy with uniaxial compressive strength (UCS), but 3.4 times higher than PDC cutter in Richard et al. (2012)'s work. The result also suggests a constant proportion between contact stress associated with matrix/rock interface and gradient of Regime II when plotted in $w-d$ space. The investigation leads to estimate uniaxial compressive strength from drilling data. With a reasonable approximation of the coefficient of friction associated with the matrix/rock interface, the predicted UCS can be a reliable estimation of the actual UCS.

Contents

List of Figures

Chapter 1

Introduction

1.1 Background

Mining exports have been the most substantial support to the Australian economy over the last decade and has contributed to about 11% of Australian GDP in 2019-20. This undoubtedly highlights the importance of the mining industry in Australia. However, although total mining expenditures have climbed up over the years, money spent on greenfield exploration has been rather conservative. As a result, many programs have been undertaken to attract more investments in greenfield exploration, such as MinEx CRC, targeting to explore new mineral deposits at depths greater than 1000 meters within Australia.

Mining involves multi-stage comminution processes to separate the precious metals from the waste rock. The processes include blasting, crushing, grinding. (Huband et al., 2005) The total amount of comminution energy (12.2 PJ in 2008/2009 in Australia) (1 $PJ = 1\times 10^{15}$ J) (Ballantyne et al., 2012) is estimated to account for up to 3% of all electrical power generated in the world, with specific comminution energy ranging from 1 (Uranium) to 2×10^5 kWh/ton (Gold). (Battelle Memorial Institute. Columbus, 1975) The total energy devoted to comminution can account for more than 50% of mining energy consumption and 10% of the total production cost. (Napier-Munn et al., 2012)

It is commonly accepted that the efficiencies of the comminution process are relatively low, as low as 1% (Lowrison, 1974; Fuerstenau and Abouzeid, 2002), and strongly dependent on rock-ore properties. The design of equipment can increase efficiency and decrease cost. An effective comminution design can bring significant dividends in downstream processing and reduce energy footprint and operating costs. It is also not uncommon for comminution circuits to fail in the case of complex ore mineralogy. The heterogeneity in rock hardness prevents comminution equipment from yielding target particle size distribution, ultimately resulting in poor liberation of wanted particles or higher unit costs in terms of energy. (Bearman, 2013)

Depending on the comminution mechanism used, mining engineers require various rock properties to come out an efficient comminution design. The industry relies on various laboratory tests such as rod, ball mill, uniaxial compressive strength, point load, drop weight, and Brazilian tests. These tests share common shortcomings such as time, sample preparation, bias in plug selection cost, repeatability, and sample amount to ensure reliable estimate. (Mwanga et al., 2015; Bearman et al., 1997)

Researchers have attempted to derive rock mechanical properties from drilling data to overcome these shortcomings, as numerous holes are drilled in the exploration phase, potentially mapping the distribution of rock strength in 3D throughout the ore mass. A large body of work focuses on empirical relations between rock properties and the rate of penetration. (Maurer, 1966; Paone et al., 1966b; Zoeller, 1974; Thuro, 1997; Kahraman et al., 2003; Mostofi et al., 2011; Mellor, 1972; Rabia, 1982)

There are, however, numerous shortcomings with such an approach. The authors often assume measurements carried on the surface are representative of the processes taking place at the bit-rock interface with little if any considerations for frictional losses between the drill string and the borehole or effect of drill rod compliance. (Elsayed and Raymond, 1999) Also, the lack of models to support

the correlation means that the effect of bit design or state of wear is not accounted for in the correlation, which means that the performance of a new or worn bit can lead to a different estimate of rock strength while drilling the same formation. (Doshvarpassand et al., 2017)

This research intends to develop a methodology to derive the rock strength (uniaxial compressive strength) from drilling data recorded while coring with diamond bits. I carry out controlled drilling experiments on a state of the art laboratory equipment and interpret the recorded data within the framework of a phenomenological model of the bit-rock interface that accounts for the fragmentation/cutting process but also the frictional losses occurring at the bit-rock interface due to wear or spurious contact between rock debris and the bit body (Detournay and Defourny, 1992; Franca et al., 2015). I run experiments on 11 different quarry rock materials, including sedimentary and hard crystalline rock, intending to derive the intrinsic specific energy of the rock (or the energy required to drill a unit volume of rock with no frictional loss) and compare (correlate) the derived intrinsic specific energy with the rock uniaxial compressive strength.

1.2 Literature Review

It is pretty common and intuitive to relate the drilling rate of penetration to the rock strength; as the rock strength increases, one expects the rate of penetration to decrease. Many authors perform statistical analyses between standard drilling data such as rate of penetration but also weight-on-bit or torque with mechanical rock properties. Paone et al. (1966a) conducted one of the earliest drill-ability studies processing raw drilling data of surface bits and impregnated diamond bits with multi-variate regression analysis. The analysis related rock properties such as Young's modulus, abrasiveness, quartz content, and rock strength to drilling rate. Other researchers (Kahraman et al., 2003; Gstalder and Raynal, 1966) have also performed correlations on rotary drilling data with tri-cone and percussive drilling data with rock properties with evidence of a negative correlation between

penetration rate and rock hardness. Thuro (1997) reported that the penetration rate for percussive drilling is also affected by lithological characteristics, such as dip angle. However, such an empirical approach overlooks other factors affecting the drilling response and thus drilling data - such as bit design, state of wear, and vibrations (Halsey et al., 1986; Murray and Cunningham, 1955; Kennedy and Spray, 1992; Sharma and Wunderlich, 1987). For example, a worn bit can yield similar WOB and TOB readings while drilling a soft rock than a sharp bit would be drilling a harder rock. Bourgoyne and Young (1974) showed a multi-variate regression model on roller cone drilling data that formation strength and bit wear affect penetration rate. Also, another shortcoming of statistical study without a priori model lies in their intrinsic sensitivity to data quality.

Other researchers have proposed models of the bit-rock interaction that relate operating parameters (WOB, TOB) and rock-related parameters (UCS) to the rate of penetration for given rock and bit properties. Warren (1987) developed a model that predicts the penetration rate of a roller cone bit based on dimensional analysis with drilling parameters and rock strength. Winters et al. (1987) extended Warren's model to consider rock ductility and bit design (cone offsets). The authors introduce several ad-hoc constants and derive the model with the intent of predicting trends in drilling performance rather than infer rock properties. Eronini et al. (1982) proposed a set of ordinary differential equations to estimate drilling rates with weight on bit, differential mud pressure, and rotary speed. The model used a 'rock constant' to address an overall rock effect on axial force and was validated on coarse sandstones. For polycrystalline diamond compact cutters, it is commonly assumed that the cutting force acting on a PDC cutter is proportional to the cross-section area of the groove traced by the cutter and the rock strength (Detournay and Defourny, 1992; Akbari et al., 2014; Cheatham and Daniels, 1979; Chen et al., 2016; Dagrain et al., 2001; Gerbaud et al., 2006; Glowka, 1985; Sinor and Warren, 1987; Zijsling, 1987). The relation between force and cross-section area of the groove traced by the cutter extends

to drill bit into a relation between torque or weight-on-bit and depth of cut per revolution.

The term strength often refers to an apparent rock strength related to a standard measure of the rock strength - such as the uniaxial compressive strength - but also affected by the cutter/groove geometry, cutter inclination, and both mud and pore pressures. Richard et al. (1998) analysed apparent rock strength with an ideally sharp cutter under atmospheric conditions at back rake angle between 5 and 20 degrees. A rock-dependent parameter was isolated and named specific energy is found very well correlated to the rock uniaxial compressive strength. Sufficient experimental evidences suggest that rock strength (at least apparent strength) can be derived from drilling data for PDC bit assuming the driller can vary the depth of cut per revolution.

Impregnated diamond bits have received much less attention than roller cone and PDC bits, with most focused on low-thrust drilling of sedimentary rock. In 1976, Peterson (1976) proposed a rate of penetration model of impregnated diamond bits based on an equivalent blade concept; similar to Hareland's work, WOB is considered a function of rock strength and cutting area. Ziaja and Miska (1982) revised Peterson's model by introducing a term to characterize the worn volume of the diamond cutter with the work performed by the bit. However, the model overlooks frictional loss due to the contact between matrix and rock. He et al. (2020) proposed a force response model for a single diamond with Coulomb-Terzaghi failure criteria that include rock strength property.

Franca et al. (2015) proposed a model for the drilling response of impregnated diamond bit inspired by Detournay and Defourny (1992)'s work. The FM (Franca-Mostofi) model assumes the drilling action of ID bit involves two independent processes: cutting and friction. They reduced the bit to a single equivalent blade of radius an outer r_o and inner r_i, radii with a cutting surface and a wear surface; more precisely, two wear surfaces, one associated with the wear of diamonds and one associated with contact between the bit matrix and rock debris.

The equivalent lengths of those two surfaces can be written as:

$$\ell_m = \frac{A_m}{r_o - r_i}; \quad \ell_d = \frac{A_d}{r_o - r_i}$$

where A_d is the sum of all the wear flats (on diamonds) and A_m the total surface area between rock and matrix. He introduced scaled a scaled torque (t) and scaled weight (w) as:

$$t = \frac{2T}{r_o^2 - r_i^2}; \quad w = \frac{W}{r_o - r_i}$$

That can be expressed as

$$t = t_c + t_{f_m} + t_{f_d}; \quad w = w_c + w_{f_m} + w_{f_d}$$

where the subscripts 'c' and 'f' distinguish the amount of torque and weight spent in the pure cutting and frictional contact process, respectively. The subscripts 'm' and 'd' denote the relative interface with the rock during cutting, with 'm' for matrix-rock contact and 'd' for diamond wear flat-rock contact, respectively. As the name 'impregnated diamond' suggests, the ID bit consists of synthetic diamonds embedded and sintered in a tungsten carbide matrix. Frictional contact occurs along diamonds' wear surface and across the contact between rock or rock debris and the matrix (three-body abrasion). The term associated with pure cutting (subscripted with 'c') can be linked to the concept of intrinsic specific, the energy ε (Teale, 1965) or the energy required to cut a unit volume of rock with an ideally sharp tool. The scaled torque and weight read:

$$t_c = \varepsilon_t d; \quad w_c = \zeta \varepsilon_t d$$

where ζ characterizes the inclination of the pure cutting force on the cutting face of diamonds. It is worth mentioning that intrinsic specific energy (ε) is different from specific energy (E), the total energy required to drill a unit volume of rock – including the energy loss not associated with any rock removal. The latter

accounts for wear, ε is only equal to E for a perfectly sharp cutter. Few researchers attempted to correlate E with rock strength, Rabia (1982); Franca et al. (2015); McFeat (1977); Tiryaki and Dikmen (2006); Yaşar et al. (2011) found that tool geometry yielded different outcomes. Franca et al. (2015) introduced equivalent terms to address the frictional process on two interfaces. The terms associated with frictional losses are expressed as a function of contact stress, and friction coefficient mobilized across the contact surface:

$$t = \varepsilon_t d + \mu_m \sigma_m \ell_m + \mu_d \sigma_d \ell_d; \quad w = \zeta \varepsilon_t d + \sigma_m \ell_m + \sigma_d \ell_d$$

where σ_d and σ_m correspond to average contact stresses applied on diamond/rock

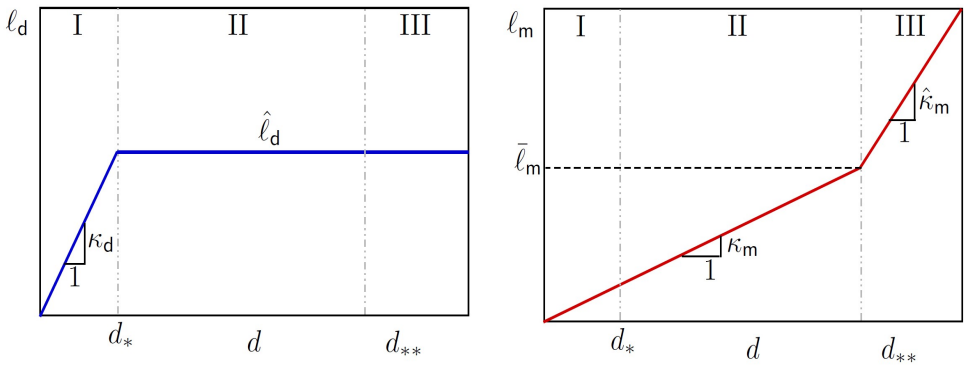

Figure 1.1: Conceptual drawings of variation of contact length in (left) diamond/rock interface and (right) matrix/rock interface.

interface and matrix/rock interface, respectively. Experimental evidence has shown that the effective contact lengths ℓ_m and ℓ_d varied with depth of cut and the authors introduced three regimes, see Figure 1.1. Regime I occurs at shallow depth of cut with all three processes increasing with depth of cut, the length ℓ_d increases until conformity between the diamond wear surfaces and the rock is established, which corresponds to the maximum contact wear flat area on diamond/rock that can be mobilized for the current bit state of war. In regime II, the length ℓ_d remains constant while matrix-rock contact still increase steadily with depth of cut until the onset of regime III where matrix-rock contact increases

faster due to inefficient evacuation of debris that leads to additional contact. A sharp rise in effective contact length between matrix/rock interface implied excessive energy consumption allocated to regrinding of debris and friction.

Regime I

$$t = (\varepsilon_t + \mu_m \sigma_m \kappa_m + \mu_d \sigma_d \kappa_d) d$$
$$w = (\zeta \varepsilon_t + \sigma_m \kappa_m + \sigma_d \kappa_d) d$$

Regime II

$$t = (\varepsilon_t + \mu_m \sigma_m \kappa_m) d + \mu_d \sigma_d \ell_d$$
$$w = (\zeta \varepsilon_t + \sigma_m \kappa_m) d + \sigma_d \ell_d$$

Regime III

$$t = (\varepsilon_t + \mu_m \sigma_m \hat{\kappa}_m) d + \mu_d \sigma_d \hat{\ell}_d + \mu_d \sigma_d \bar{\ell}_m$$
$$w = (\zeta \varepsilon_t + \sigma_m \hat{\kappa}_m) d + \sigma_d \hat{\ell}_d + \sigma_d \bar{\ell}_m$$

Regime II is most appropriate for deriving the intrinsic specific energy from these equations. However, one needs to eliminate the effect of matrix-rock contact or estimate it a priori. Mostofi (2014) showed that sandblasting or leaching of the segments increase diamond exposure and eliminates matrix-rock contact in regime I and II.

1.3 Shortcoming of past research

To summarise, drilling response models, especially for PDC cutters, mainly were looked at and validated on weak rocks, such as sedimentary rocks and are non-abrasive. However, in the context of ID drilling, due to deeper operating depths, there is a necessity to cover a broader range of rock strengths, including abrasive

materials, which not much has been done in that space. There is also limited understanding of the variation of model parameters under different rock materials for ID drilling, such as intrinsic specific energy and coefficient of friction associated with matrix/rock boundary. In my work, the interpretation of drilling response is conducted on the basis of the model from Franca et al. (2015) under the same assumptions:

1. Drilling response is composed of two independent processes: cutting and friction.

2. Cutting force is proportional to cutting area.

3. Rock property ε_t, diamond-rock properties (ζ, μ_d, σ_d), and matrix-rock properties (μ_m, σ_m) are constant for a given rock and bit.

4. The wear flat contact area associated to diamond/rock contact and matrix/rock contact are linearly proportional to depth of cut in all regimes.

In this research, I first intend to run a series of drilling experiments in both sedimentary and crystalline rocks with a sandblasted bit to derive the intrinsic specific energy, and compare to the uniaxial compressive strength. Testing very abrasive material raise challenges to maintain the effect of diamond wear during experiment negligible. For that purpose, I designed and tested a dedicated experimental protocol, the detail can be found in Chapter 2. In Chapter 3, I aim to estimate the effect of matrix-rock contact (μ_m and $\sigma_m\kappa_m$) on the drilling response with the intent to be able to account for the effect a priori and be able to derive the intrinsic specific from data recorded while drilling with standard (non-sandblasted) bit. I carry out numerous drilling experiments with sandblasted and standard bits in all the eleven rocks selected for that purpose.

Chapter 2

Methodology

2.1 Introduction

This research investigates the effect of rock strength on the drilling response of ID bits, with the intent to derive the rock strength from drilling data. The work presented in this thesis is experimental and supported by a phenomenological model of the bit-rock interface (Franca et al. (2015)). The model parameter most likely related to rock strength is the intrinsic specific energy related to the torque associated with the pure cutting process and the depth of cut per revolution. However, the model also indicates that the total torque (eventually the measured variable) is also affected by contact between matrix and rock. Therefore the challenge in deriving ε from the drilling data is to either eliminate the term due to matrix-rock contact or estimate intrinsic specific energy ε.

A complete drilling response encapsulates force responses measured on the bit at different depths of cut. I ran the drilling and cutting experiments on state-of-the-art laboratory rig, Echidna, to ascertain that the drilling response measured is accurate. The rig is equipped with a servo-control unit that accurately imposes different penetration rates. A list of high-precision sensors provides readings that are later used for depth of cut calculation. To recap, the interface laws for a

standard (subscript as N) impregnated diamond bit are:

$$t_N = (\varepsilon_t + \mu_m \sigma_m \kappa_m) d + \mu_d \sigma_d \ell_d$$
$$w_N = (\zeta \varepsilon_t + \sigma_m \kappa_m) d + \sigma_d \ell_d$$

My approach is twofold. I first ran experiments with a sandblasted bit modified to eliminate the matrix/rock contact ($\sigma_m \kappa_m$) and directly estimate the intrinsic specific energy ε and compare with the rock strength on 11 different rock materials. Due to the absence of matrix bearing surface, I assume the matrix contact term is minimised and therefore negligible ($\sigma_m \kappa_m = 0$). For a sandblasted bit (subscript as L), the interface laws read:

$$t_L = \varepsilon_t d + \mu_d \sigma_d \ell_d$$
$$w_L = \zeta \varepsilon_t d + \sigma_d \ell_d$$

The experiment covers drill tests on sedimentary and crystalline rocks, including very abrasive high quartz content igneous rock. A challenge inherent to the experiment carried out in very abrasive rocks is to minimise the effect of diamond wear on the response. I thus designed a specific experimental protocol to vary the depth of cut (necessary to map out the drilling response) fast enough to minimise the extent of wear but slow enough to make sure the response match a steady-state response.

Then, I ran a similar experiment with a standard bit to quantify the effect of matrix/rock contact on drilling response. The difference between gradients of weight response against depth of cut of a normal bit and a sandblasted bit can be used to estimate the contact term associated with matrix/rock contact, see Figure 2.7.

2.2 Echidna

Echidna is a laboratory scaled drilling rig that accommodates field-sized coring bits and full-face bits to drill 540 mm long holes, refer to Figure 2.1. The rig consists of three key components: a servo-controller rotary and a feed drive system, a mud/water circulation system, and several sensors hooked up to a data acquisition system. I ran all experiments under servo kinematic control, meaning both the feed rate and angular velocity are controlled while the data acquisition system records the forces acting on the cutting tool. The servo-control allows for high precision master-slave relation between feed and rotation control to precisely control the depth of cut per revolution with an accuracy of a few microns.

Echidna is a state-of-the-art kinematic controlled rig for drilling and rock cutting tests, respectively and has several advantages. The tests are run under controlled feed rate and bit angular velocity while the weight (normal force) and torque (tangential force) are measured while drilling (cutting). Imposed kinematics means that the response is less likely to be affected by vibrations.

The user operates the equipment via an interactive graphical interface in manual mode. The operator enters both the depth of cut and bit RPM manually at any time to form a trajectory (operating parameters invariant for a time duration). In preset mode, the rig executes a preset trajectory. The depths of cut and bit angular velocities are arranged in a timetable, also known as the feed rate profile.

Echidna is equipped with several sensors hooked up to HBM MGCPlus data acquisition system sampling data at 2.4 kHz. A force transducer measures thrust (or weight-on-bit) and generates precise measurement up to 50 kN with a non-linearity of 17.5 N. A torque sensor coupled with the rotary drive mechanism that can rotate from 0.95 to 188.4 rad/s measures torque up to 112 Nm with a non-linearity of 0.112 Nm. To confirm feed rate is correctly applied, the rig has a linear displacement sensor that measures with a precision of 0.762 $\times 10^{-4}$ m. I re-evaluate feed rate and bit angular velocity by the derivatives of linear position

and angular position of the bit with respect to time required to complete a unit bit revolution.

Figure 2.1: The laboratory scaled drilling rig, Echidna.

2.3 Rocks

I consider four igneous rocks: Bluestone granite, Austral Black, Verde Austral, and Calca Red, see Figure 2.2. Calca red (Taber Index of 133) and Austral black gabbro (Taber Index of 126) are the two most abrasive with 36% and 3% quartz content, respectively. The Bluestone granite is a fine-grained basalt with a minute quartz content. Verde austral is a green granite from Western Australia with coarse uniform grains. Austral black is a gabbro from South Australia with pale black colour due to massive crystalline plagioclase and biotite and 2.61% quartz content. Figure 2.3 shows the abundant minerals and their volume percentage.

Table 2.1 summarises mechanical properties of the rock material, uniaxial compressive strength, q, the young modulus, Y, and v the Poissons ratio, recorded during uniaxial compressive strength carried out on four samples (diameter of 25.64 mm and sample length of 49.82 mm) at CSIRO rock mechanical laboratory (see Appendix B for more details on the test results).

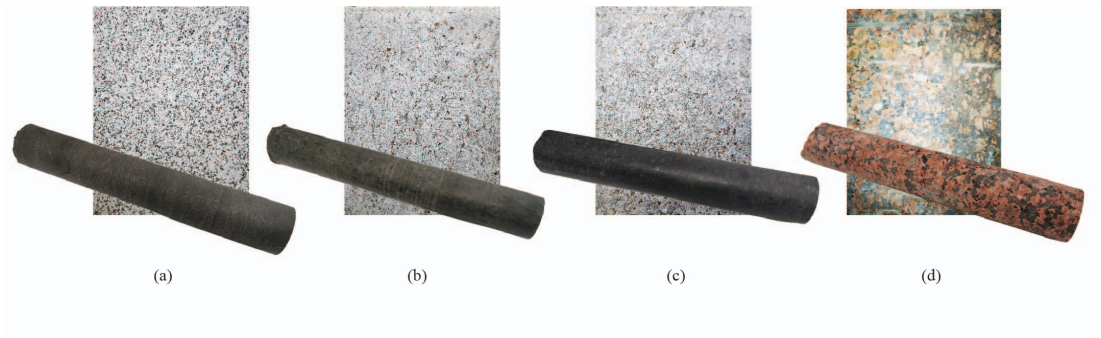

Figure 2.2: Igneous rocks used in this research, (a) Bluestone granite, (b) Verde austral, (c) Austral black, and (d) Calca red.

I used seven sedimentary rocks, both carbonates and clastics. The hardest sedimentary rock is a heterogeneous Guelph dolomite. Austin chalk is a homogeneous marl rich micro granular calcite originated from Texas, USA. Colton is a silty sandstone with a pale grey appearance and sub-rounded fine grain. The Crab orchard is a hard sandstone that originated from Cumberland Plateau in

Tennessee, with brownish streaks. 90% quartz content. Donnybrook is a fine to medium-grained feldspathic sandstone from the town of Donnybrook in Western Australia. The Grey Berea is a permeable homogeneous sandstone. Indiana limestone, also known as Salem limestone, is a homogeneous rock made of calcium carbonate (97%). I derive the uniaxial compressive strength of the sedimentary materials (see Table 2.1) from scratch tests carried on core samples on a "scratch machine" Wombat, see Figure 2.4 and Appendix A for more details.

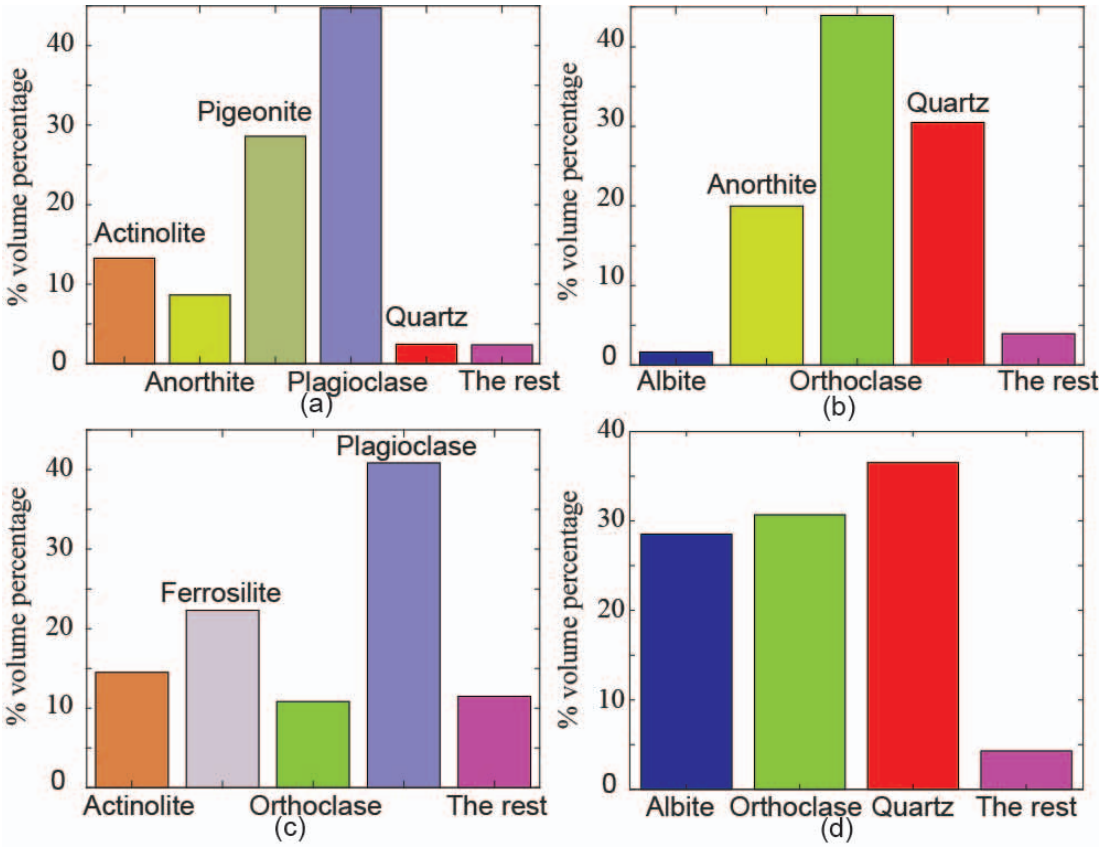

Figure 2.3: Mineral content of the igneous rocks, with (a) Bluestone granite, (b) Verde austral, (c) Austral black, and (d) Calca red.

Rock	$q\ (MPa)$	$Y\ (GPa)$	v
Verde Austral	181	43	0.15
Austral Black	170	45	0.15
Calca Red	155	37	0.28
Bluestone Granite	126	21	0.17
Dolomite	152	-	-
Crab Orchard	117	-	-
Donnybrook	72	-	-
Colton	50	-	-
Grey Berea	42	-	-
Indiana Limestone	24	-	-
Austin Chalk	11	-	-

Table 2.1: The uniaxial compressive strength derived from standard UCS test and Wombat scratch test for igneous and sedimentary rocks, respectively.

Figure 2.4: The wombat cutting rig to extract rock strength for sedimentary rocks.

2.4 ID bit and segments

I used two ID bits and one segment provided by the company HARDCORE with 15% in diamond concentration and mesh size of 25/35 (595 to 707 microns) with a matrix rated as soft, see Figure 2.5.

Figure 2.5: Impregnated diamond bit used for the research, a commercial product from Hardcore Diamond Drill Products.

I sandblasted one drill bit to remove the matrix in the vicinity of protruding diamonds and increase their exposure see Figure 2.6. The drilling responses from a standard bit and a sandblasted version bit are plotted in both t-d and w-d spaces, see Figure 2.7.

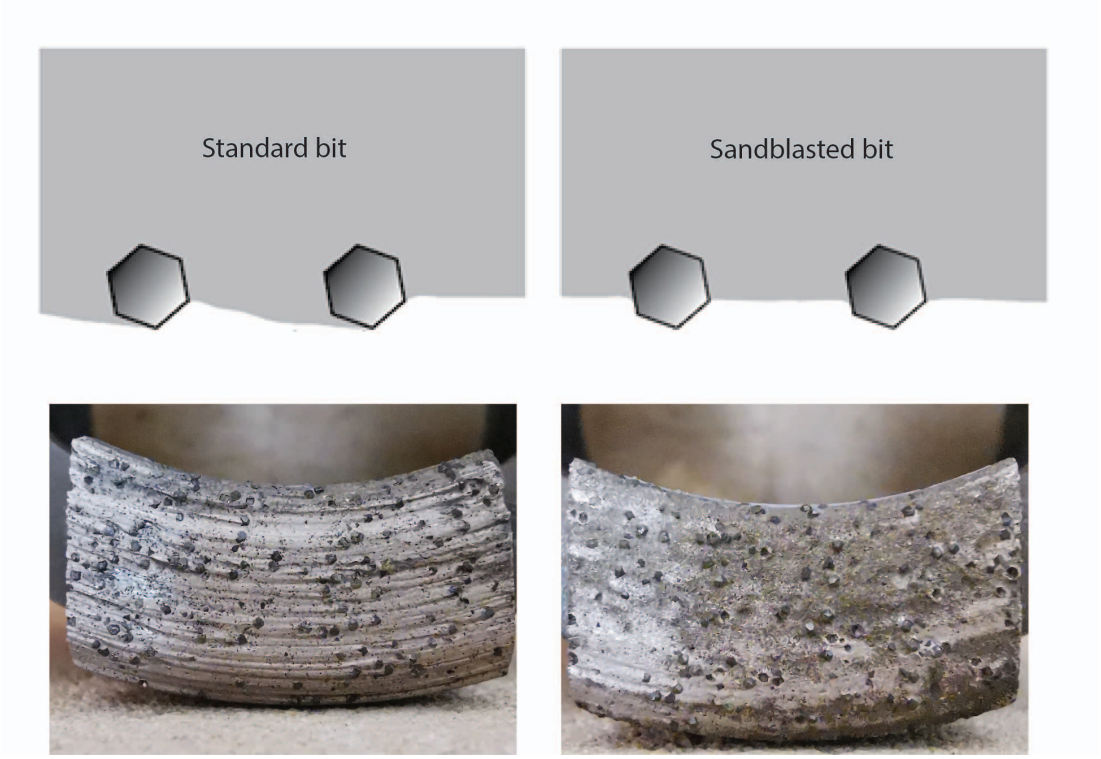

Figure 2.6: A comparison of standard bit and sandblasted bit.

From the data, I determine the extent of each regime and calculate the gradient in Regime II. The interface laws for an impregnated diamond bit in regime II read

$$t = (\varepsilon_t + \mu_m \sigma_m \kappa_m) d + \mu_d \sigma_d \ell_d$$
$$w = (\zeta \varepsilon_t + \sigma_m \kappa_m) d + \sigma_d \ell_d$$

After sandblasting the bit surface, I assume the matrix-rock contact has been cancelled out meaning ($\sigma_m \kappa_m = 0$) or

$$t = \varepsilon_t d + \mu_d \sigma_d \ell_d$$
$$w = \zeta \varepsilon_t d + \sigma_d \ell_d$$

From which I can derive the intrinsic specific energy ε as the gradient in the $t - d$

space in regime II. I derive the coefficient ζ as the ratio of the gradients from the $w-d$ and $t-d$ space, respectively, and then compute the term $\sigma_m \kappa_m$ from the gradients in the space w_d in Regime II.

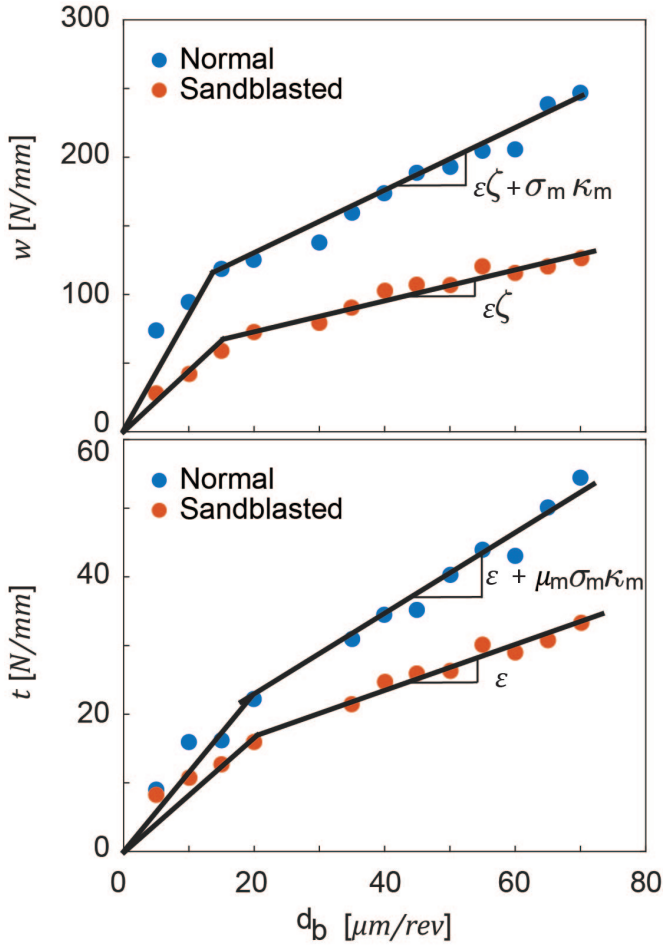

Figure 2.7: Scaled weight and torque response vs depth of cut for test carried out on Bluestone granite for a standard bit and a sandblasted bit. The term associated with matrix/rock contact is the difference between the gradients in Regime II.

I derive the matrix/rock contact parameters (μ_m) with drilling response of the standard and sandblasted bits. The coefficient of friction measured here resembles the analytical solution based on the Franca-Mostofi model of bit/rock interface laws. The coefficient of friction associated with matrix/rock contact is

not well-understood, with previous studies suggesting the frictional process is of three-body contact. The coefficient of friction can read as

$$\mu_m = \frac{\nabla(t-d)_{normal} - \nabla(t-d)_{sandblasted}}{\nabla(w-d)_{normal} - \nabla(w-d)_{sandblasted}}$$

with ∇ is the gradient measured in scaled torque versus depth of cut $(t-d)$ and scaled weight $(w-d)$ space, respectively.

2.5 Experimental procedure

The first constraint imposed on our experimental protocol is to minimise the effect of diamond polishing on the drilling cutting response over the duration of the test, which can be quite pronounced in the most abrasive rock such as Calca red. I first conducted drilling experiments in both Calca red and Bluestone granite at a constant depth of cut ($d_b = 110\ \mu m/rev$) and angular velocity ($\Omega = 400 RPM$) while monitoring the weight and torque. Figure 2.8 shows the evolution of the

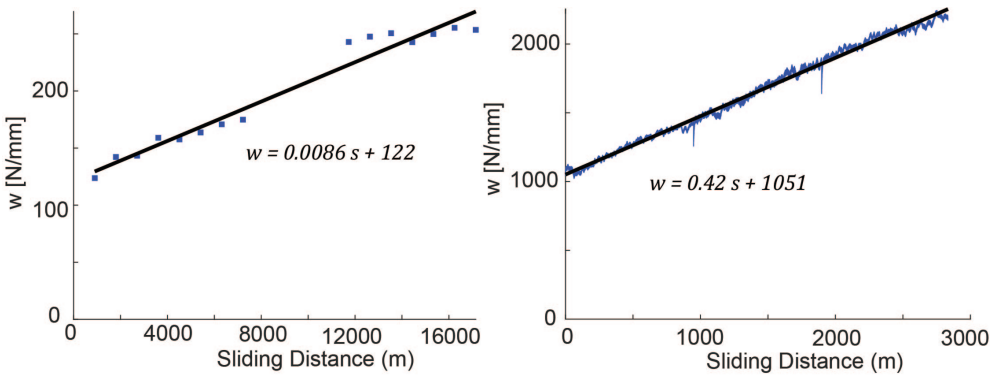

Figure 2.8: Variation of scaled weight with respect to sliding distance, to cut Bluestone granite (left) and Calca red (right) at $d_b = 110\ \mu m/rev$ and $\omega = 2.58\ ms^{-1}$

weight with the linear distance travelled by the segments on the bit face, as diamonds are polishing. I consider that the effect of polishing can be neglected if its contribution (in terms of weight or torque) is less than 5% over the duration of a drilling test. If we assume the weight mobilised along diamond wear surface

can written as

$$w_{f_d}(s) = \eta s$$

we can express the maximum travelling distance

$$s_* = \frac{0.05\bar{w}}{\eta}$$

Where s_* means the critical sliding distance when the effect of polishing increases the mean weight $\bar{w}$ by 5%. From the results shown in Figure 2.8, it means that tests should not exceed a critical sliding distance s_*, of about 125 m in sliding distance for the most abrasive material (Calca Red). For all drill tests, the bit rotates at 400 RPM, so the duration of the test that corresponds to a sliding distance s_* reads

$$\tau_* = \frac{60 s_*}{2\pi \bar{r} \Omega}$$

where $\bar{r} = \frac{r_o + r_i}{2}$. For a NQ size core bit, I have $\tau_* = 48s$.

As shown earlier, I need to vary the depth of cut over a reasonable range in order to build the bit drilling response and extract the intrinsic specific energy. Commonly, we build the drilling response by increasing the depth of cut per step where each step lasts several bit revolutions (typically a minimum of 10 to 20) over which I can compute a reliable average of the forces. The procedure was challenging in capture drilling response of abrasive rocks. Experimental results have shown that equivalent contact wear length of diamond/rock interface increases over the duration of the drill test, the drilling response became unrepresentative.

I therefore consider test with a continuous variation of depth of cut, but would like to make sure that the relative error or change in depth of cut over a bit revolution remains a constant α and independent of the mean depth of cut, meaning

$$\dot{d} = \alpha d$$

where the dot represents the derivative with respect to time τ, which leads to

$$d = d_o e^{\alpha\tau}$$

with d_o the initial depth of cut. I now apply our two constraints namely (i) a maximum difference of Δd in the depth of cut over 20 bit revolutions (in previous method the maximum difference $\Delta d = 0$ as same depth of cut lasts several bit revolutions) and (ii) a maximum sliding distance s_*.

The first constrain is introduced to make sure the drill test remains under kinematic control, where acceleration $\dot{V}$ to have slow variation. The upper boundary allows one to explore the complete drilling response over a representative time window, which I have selected a time window equivalent to 20 revolutions ($n = 20$) when the bit is set to rotate at 400 RPM. Detournay et al. (2008) suggests the subsequent rate of penetration should not exceed more than 5% compared to the current value after the time required to complete n revolutions. With a maximum variation in depth of cut of less than 5% over n revolutions, the error in depth of cut reads

$$e_n = \frac{\dot{d}_{\tau_n}}{d} = \alpha\tau_n$$
$$e_n = \frac{2\pi\alpha n}{\Omega} <= 0.05$$

which means

$$\alpha <= \frac{0.05\Omega}{2\pi n}$$

The lower boundary relates to the maximum sliding distance criteria, I consider the depth of cut increases over the duration of the test τ_* from d_o to maximum depth of cut d_*

$$d_* = d_o e^{\alpha\tau}$$

$$\alpha >= \frac{1}{\tau_*} ln \frac{d_*}{d_o}$$

The constant is found to fall between 0.0694 and 0.16 for a bit to increase from

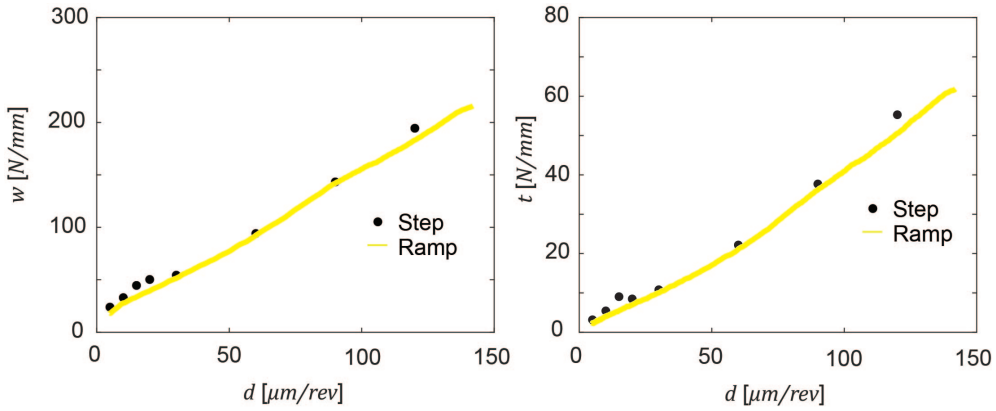

Figure 2.9: Drilling response for test carried out with the depth of cut increased by steps and by exponential ramp ($\alpha = 0.1$) on Donnybrook sandstone. The ramp tests lasts 29 seconds to ramp up from $d_b = 5$ to 140 $\mu m/rev$

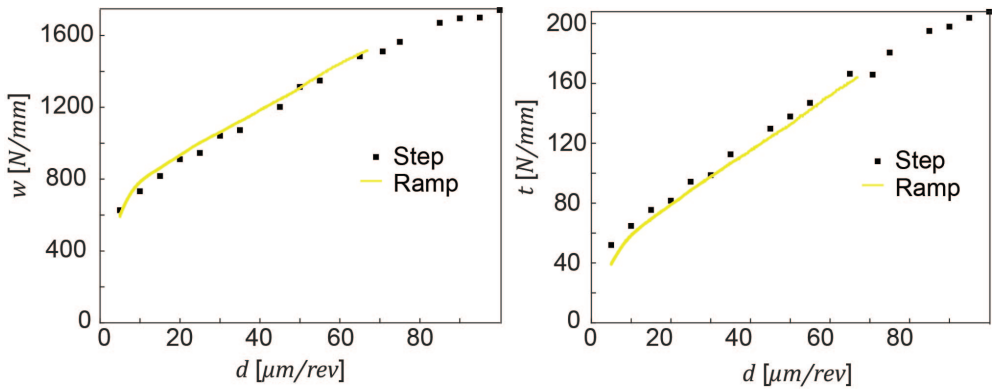

Figure 2.10: Drilling response for test carried out with the depth of cut increased by steps and by exponential ramp ($\alpha = 0.1$) on Calca red. The ramp tests lasts 29 seconds to ramp up from $d_b = 5$ to 140 $\mu m/rev$

$d_b = 5$ to 140 $\mu m/rev$ at 400 RPM (and $n = 20$). Figure 2.9 and 2.10 show the drilling responses for tests carried out in Donnybrook sandstone and Calca red with continuous variation of depth of cut with α =0.1.

To summarise, I operated a state-of-the-art laboratory scaled drilling rig, Echidna to perform drilling activities. The drill campaign encompassed eleven rock materials of various rock properties drilled with two impregnated diamond bits of different surface topology, a standard and a modified-sandblasted bit. The drill test used a dedicated drilling profile to capture drilling response of a range of depth of cuts. Drilling data were processed and interpreted by plotting it in various space, which will be discussed in Chapter 3.

Chapter 3

Results and Discussion

3.1 Intrinsic specific energy and UCS

First the eleven rock samples were drilled under the atmospheric condition on Echidna with the sandblasted bit. The results show that the onset of regime II occurs at a depth of cut of about 10 $\mu m/rev$. I apply a best linear fit to the pair $t - d$ in Regime II (shown as dashed line in the Figure 3.1), as the equations mentioned in Chapter 2 suggest the gradient represents the intrinsic specific energy ε_t.

$$t = \varepsilon_t d + \mu_d \sigma_d \ell_d$$
$$w = \zeta \varepsilon_t d + \sigma_d \ell_d$$

Figure 3.2 and Table 3.1 compare the derived intrinsic specific energy ε with the uniaxial compressive strength of the rock, q. The figures also includes earlier data from Franca et al. (2015).

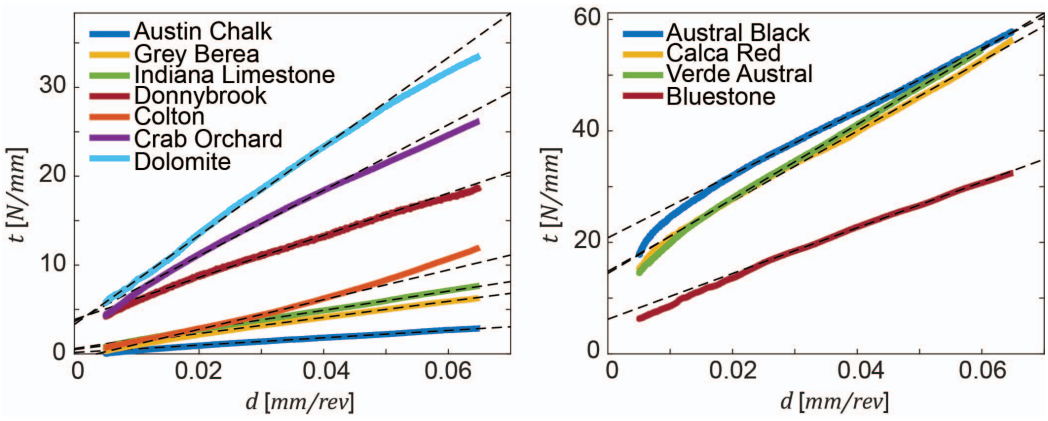

Figure 3.1: Evolution of the scale torque with depth of cut for both sedimentary (left) and igneous (right) rocks.

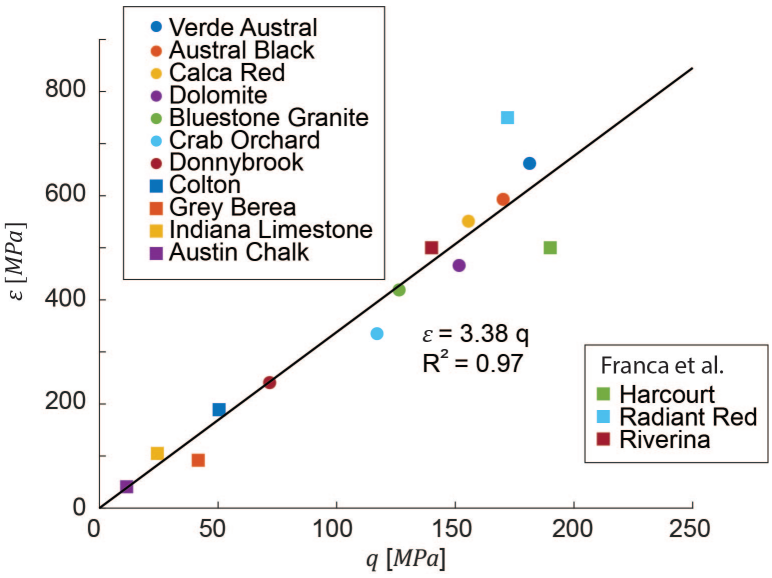

Figure 3.2: Intrinsic specific energy (MPa) versus uniaxial compressive strength (MPa)

The results reveal a strong linear correlation between intrinsic specific energy and uniaxial compressive strength, with a correlation of determination (R squared) of 0.97, which demonstrates the potential to derive rock strength from drilling data recorded while drilling with a diamond bit.

Rock	q	ε	ζ	μ_m	$\sigma_m \kappa_m$	(E)	(S)
Radiant Red	172	750	4.0	-	-	3000	-
Verde Austral	181	662	4.0	0.18	4604	1473	7243
Calca Red	170	593	3.4	0.13	3761	1092	5805
Austral Black	155	551	3.2	0.30	2641	1334	4760
Harcourt	190	500	2.8	-	-	1400	-
Riverina	140	500	2.8	-	-	1400	-
Dolomite	152	466	2.8	0.21	1408	768	2906
Bluestone Granite	126	419	2.8	0.16	1163	603	2330
Crab Orchard	117	335	3.3	0.17	851	479	1948
Donnybrook	72	241	3.0	0.06	794	291	1514
Colton	50	189	2.1	0.16	433	260	836
Grey Berea	42	92	2.3	0.17	248	137	471
Indiana Limestone	24	105	2.3	0.29	231	168	458
Austin Chalk	11	41	0.7	0.53	45	65	72

Table 3.1: The measured variables from drilling experiment.

3.2 Inclination

The inclination is referred to as the direction of cutting force, represented as the ratio between the normal force to the tangential force, which both measured independently. The inclination is denoted as ζ in the drilling response model, and can express in angle:

$$\zeta = tan(\phi)$$

where ϕ is the inclination angle which is reported to be a function of rock properties such as friction angle under Mohr-Coulomb criterion and bit properties such as back rack angle. From the sandblasted results, I further derive the coefficient ζ from the linear fit between the pair $w - t$ in Regime II, see Figure 3.3 and Figure 3.4.

$$w = \zeta t + \sigma_d \ell_d (\mu_d - 1)$$

The results are summarised in Table 3.1.

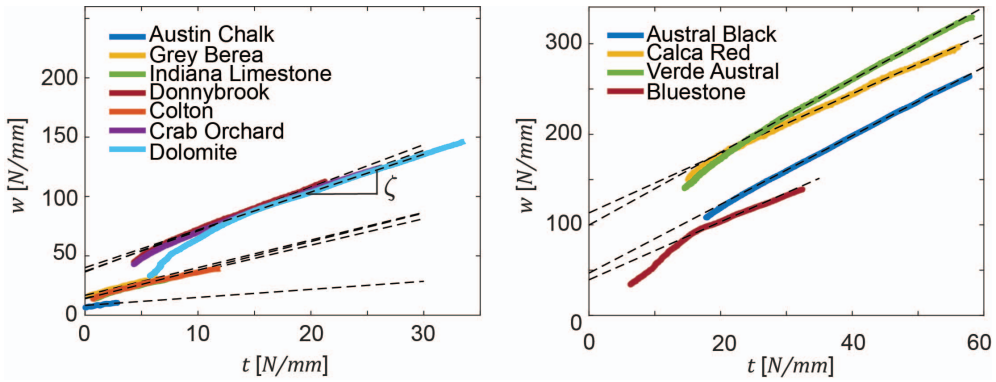

Figure 3.3: Scaled weight versus scaled torque.

Figure 3.4 depicted the inclination angle measured on various rocks. It is observed the inclination in ID drilling is generally larger than one obtained from PDC in most rocks, with Detournay et al. (2008) reported ζ in the range of 0.5 to 0.8. However, in practical application (standard bits), the term associated with matrix-rock contact ($\mu_m \sigma_m \kappa_m$) cannot be eliminated. Therefore, the next section explores how to estimate and eventually predict the term associated with matrix-rock contact.

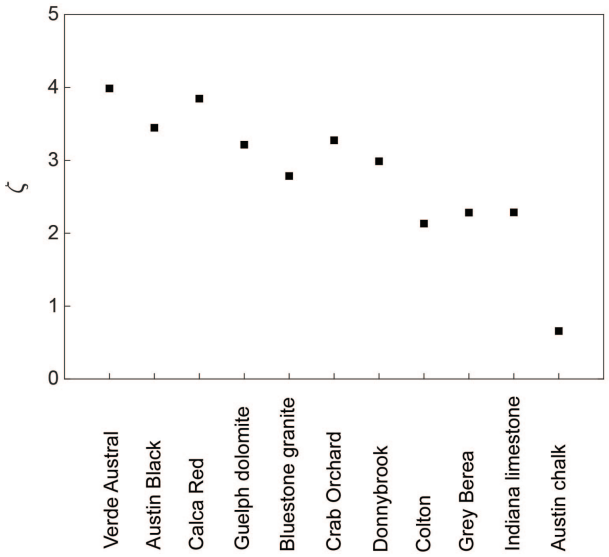

Figure 3.4: Zeta calculated on various rocks arranged from highest UCS to lowest UCS, from left to right.

3.3 Matrix/rock contact term

I carried out a similar drilling test with a standard bit (not sandblasted) and compared the results of tests carried out with the sandblasted bit, see Figure 3.5 and Figure 3.6.

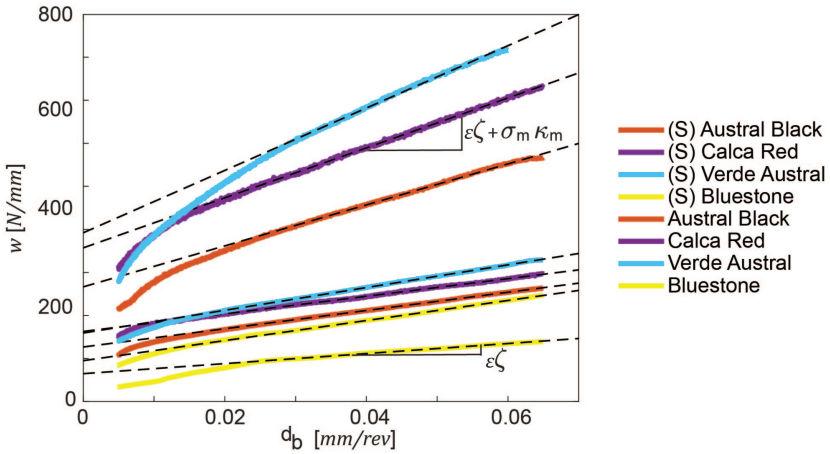

Figure 3.5: Scaled weight response of a normal bit and a sandblasted bit (S) on igneous rocks.

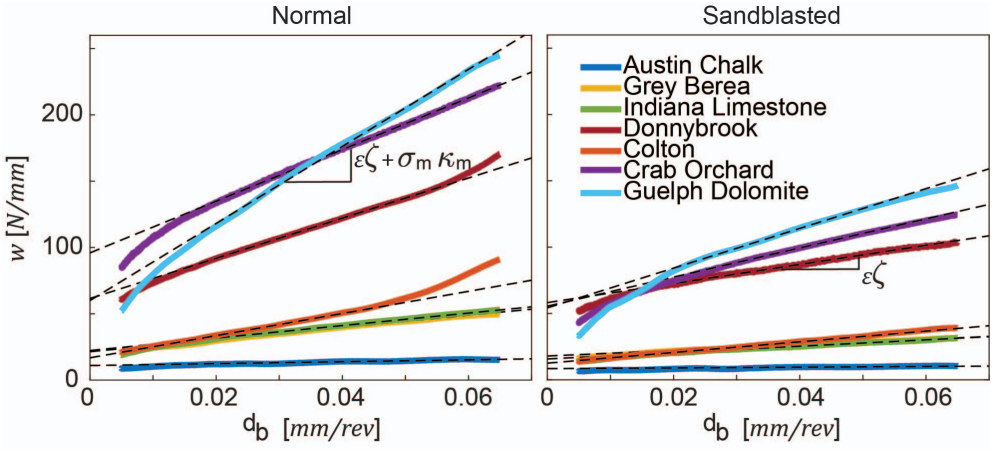

Figure 3.6: Scaled weight response of a standard and sandblasted bit on sedimentary rocks.

From the linear fit carried out on both data sets (standard and sandblasted) in regime II, I derive the terms $\sigma_m \kappa_m$ as the difference between the slopes for a

standard bit ($\zeta\varepsilon + \sigma_m\kappa_m$) and sandblasted bit ($\zeta\varepsilon$).

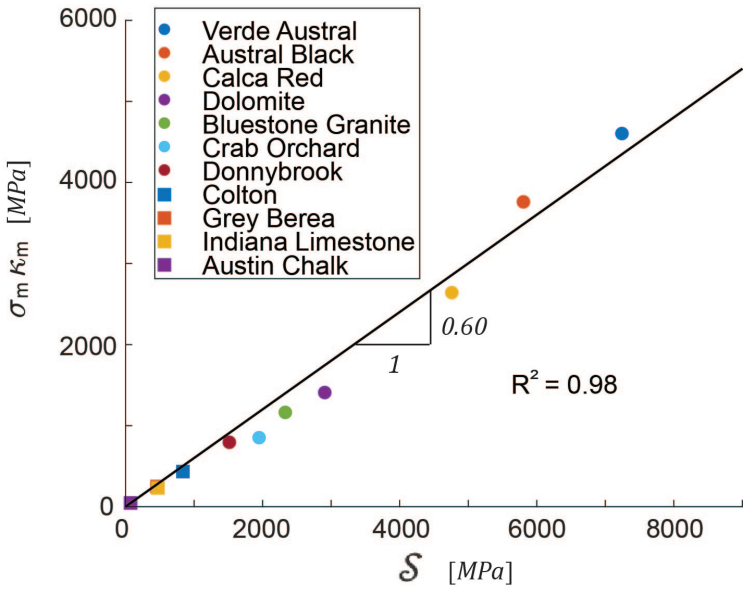

Figure 3.7: Matrix/contact stress term versus scaled weight gradient of normal bit.

The term $\sigma_m\kappa_m$ is found to correlate well with the weight gradient of the standard bit ($\zeta\varepsilon+\sigma_m\kappa_m$), see Figure 3.7. For simplicity I introduced new variable as the gradients in Regime II in both $t-d$ and $w-d$ spaces from both standard bit as follow

$$\mathcal{E} = \varepsilon + \mu_m\sigma_m\kappa_m$$

$$\mathcal{S} = \zeta\varepsilon + \sigma_m\kappa_m$$

The intrinsic specific energy therefore can be written as

$$\varepsilon = \mathcal{E} - \mu_m\sigma_m\kappa_m$$

As shown earlier that I can approximate the term $\sigma_m\kappa_m$

$$\sigma_m\kappa_m = 0.60\mathcal{S}$$

and from the correlation between unconfined compressive strength, q and intrinsic specific energy I have

$$q = \frac{1}{3.38}\varepsilon = 0.30\varepsilon$$

By combining the last three equations, I can derive UCS as

$$q = 0.30(\mathcal{E} - 0.60\mu_m\mathcal{S})$$

where $\mathcal{E}$ and $\mathcal{S}$ are the gradient in regime II in the $t - d$ and $w - d$ space, respectively.

The proposed equation above requires an estimate of the coefficient of friction associated with matrix/rock contact. It is worth mentioning that the coefficient of friction includes both two-body and three-body abrasions. The results of the two-body abrasion test suggest that the mean coefficient of friction is weakly sensitive to rock properties, with an average of about 0.33 across different rocks, see Appendix C. The actual coefficient of friction, which involves both two body abrasion and three body abrasion can be measured by

$$\mu_m = \frac{\mathcal{E} - \varepsilon}{\mathcal{S} - \zeta\varepsilon}$$

The coefficient of friction derived with drill test drilling response encapsulates the friction coefficient associate with matrix/rock contact and three-body contacts: rock, cutting, and matrix. It is observed that coefficients of friction associated with three-body contact are lower than two-body contact. The average coefficient of friction is 0.17, see Figure 3.8.

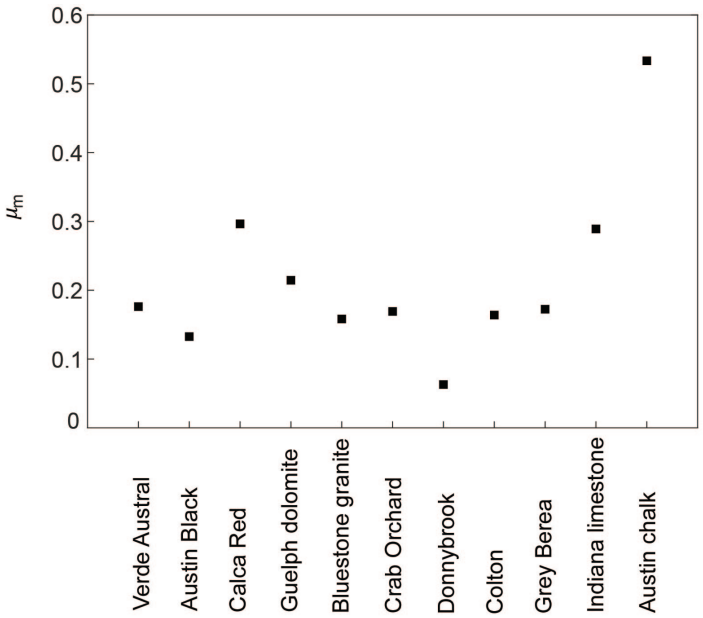

Figure 3.8: Coefficient of friction associated with matrix/rock contact measured from drill tests.

The actual unconfined compressive strength, q (MPa) is compared with the value estimated using the equation above, with μ_m derived from $\mu_m = \frac{\mathcal{E}-\varepsilon}{\mathcal{S}-\zeta\varepsilon}$ or $\mu_m = 0.17$, shown as the bottom and top plot of Figure 3.9 respectively. The mean error is found close to 30% based on available eleven rock samples with a standard deviation of 0.2 when μ_m is 0.17. The error decreases with a good estimation of the coefficient of friction associated with matrix/rock contact, using the drilling data obtained from the drill test, the mean error is 10% with a standard deviation of 0.1. For example, consider the coefficient of friction for Calca red as 0.3, as shown in Figure 3.9, the estimated strength is 146 MPa while the actual strength is reported to be 156 MPa.

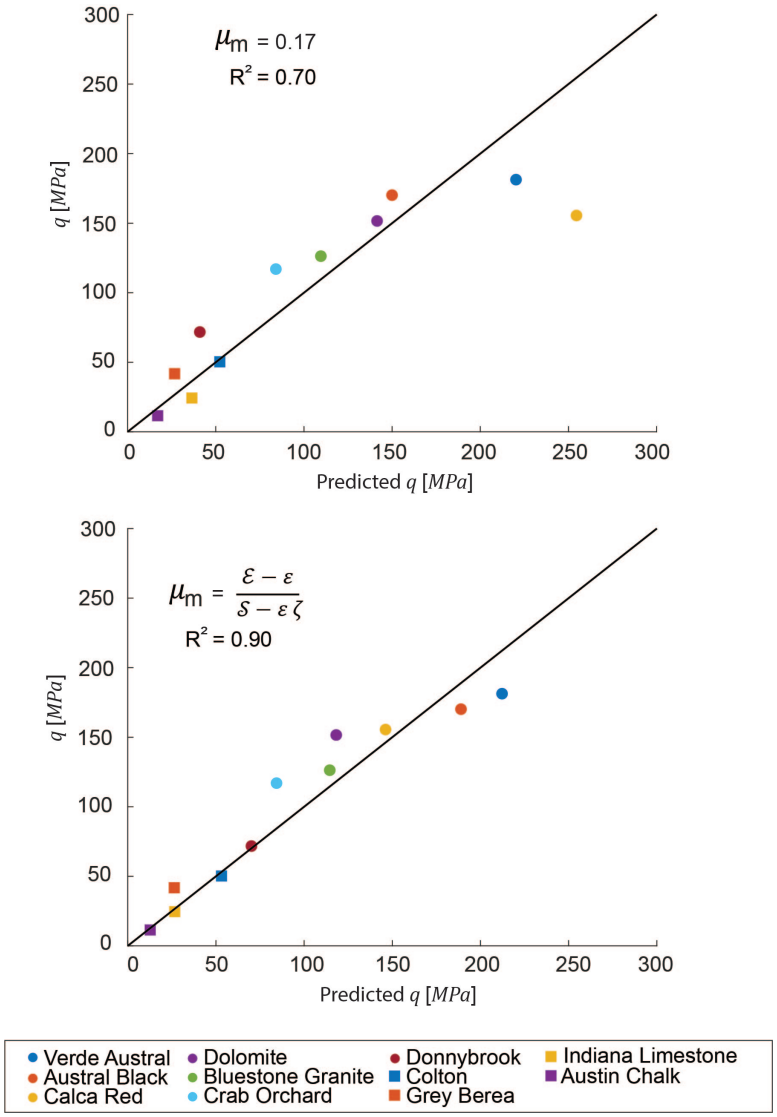

Figure 3.9: Dispersion between actual and estimate unconfined compressive strength, at $\mu_m = 0.17$ (top) and μ_m from Figure 3.8 derived with drilling data (bottom).

Chapter 4

Conclusion

In this work, I carried out extensive laboratory atmospheric drilling experiments with diamond core bits on 11 different rock materials, 7 sedimentary and 4 igneous rocks that cover a wide range of strengths (uniaxial compressive strength from 4 to 180 MPa) and abrasiveness. UCS were determined under standard testing or a WOMBAT scratch test for igneous rocks and sedimentary rocks, respectively, on rock core samples which are by-products of the drill tests.

I ran the test on a dedicated electric servo-control laboratory rig operated under precise kinematic control with both feed rate and angular velocity precisely set while the axial thrust (weight-on-bit) and torque are recorded with high accuracy. The servo-control means I achieve a precision of a few microns on the controlled depth of cut.

I implemented a specific experimental protocol that consists in increasing the depth of cut continuously as an exponential function of time. The rate of change of the depth of cut was selected so that (i) the effect of diamond polishing had a negligible effect on the drilling response over the duration of the experiment and (ii) the relative variation of depth of cut over 20 bit revolutions was less than 5%, where 20 bit revolutions is the duration over which drilling parameters were averaged to yield a reliable measurement.

The results show that the intrinsic specific energy derived from drilling data

is very well correlated to the uniaxial compressive strength of the rock ($\varepsilon = 3.4q$). The intrinsic specific energy is the coefficient of proportionality between the scaled torque ($t = \frac{2T}{a^2}$) and the depth of cut per revolution for a bit that has been sandblasted so that the contact between matrix and rock is negligible, as sandblasting wears away some of the matrix surrounding the exposed diamonds in particular the so called comet tails trailing behind the diamond in the direction of cutting.

Although the results are very promising, the practical application requires us to extend the analysis to standard bit configuration (i.e. active comet tails). For that purpose, I carried out identical drilling experiments with both sandblasted and standard bits, in each rock material.

By comparing the results, I show that the term associated with rock-matrix contact can be approximated reasonably well as proportional to the intrinsic specific energy. As a result, the intrinsic specific energy and thus the rock strength can be derived from the drilling response of diamond core bit with the additional assumption that the coefficient of friction between rock and matrix can be considered independent of the rock material and equal to 0.17.

The results are very promising, although they rely on the hypothesis that the friction coefficient is very weakly dependent on the rock.

Future work should first focus on extending the correlation between ε and q to more materials and in particular ore material, and possibly different bit types. Specific effort should be dedicated to refining the friction coefficient estimate μ_m and exploring how it varies with the matrix hardness.

Finally, to apply the method to field data, one needs first to derive an estimate of the torque, weight and depth of cut at the bit from surface measurement of torque, force, rate of penetration and angular velocity. This means estimate frictional losses between the surface and the bit and account for the effect of the drill string compliance.

Appendices

Appendix A

Wombat Scratching Test

Austin Chalk

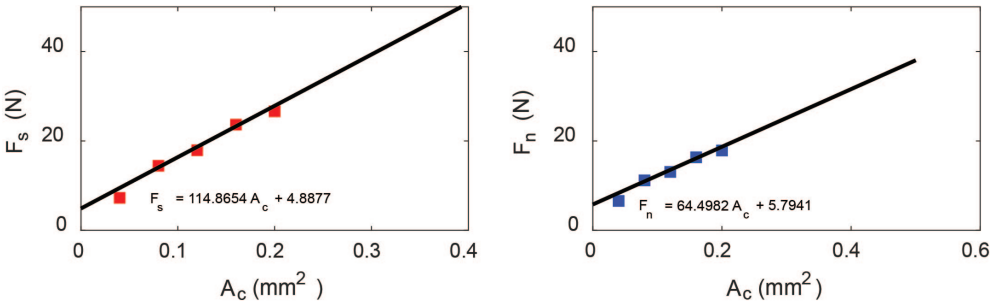

Figure A.1: The tangential force and normal force response of Austin Chalk.

Colton Sandstone

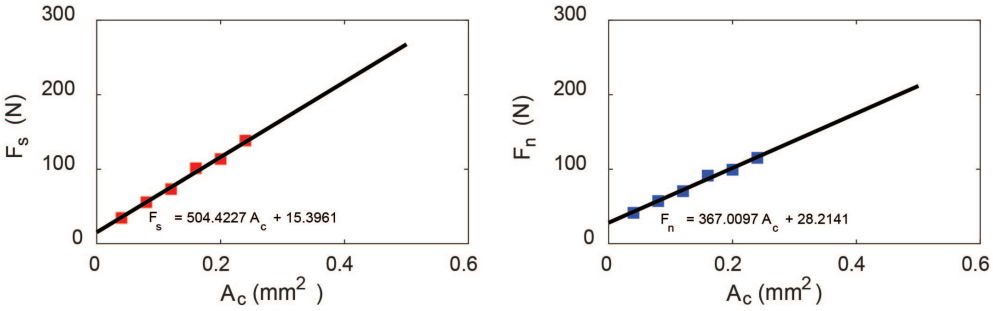

Figure A.2: The tangential force and normal force response of Colton sandstone.

Crab Orchard Sandstone

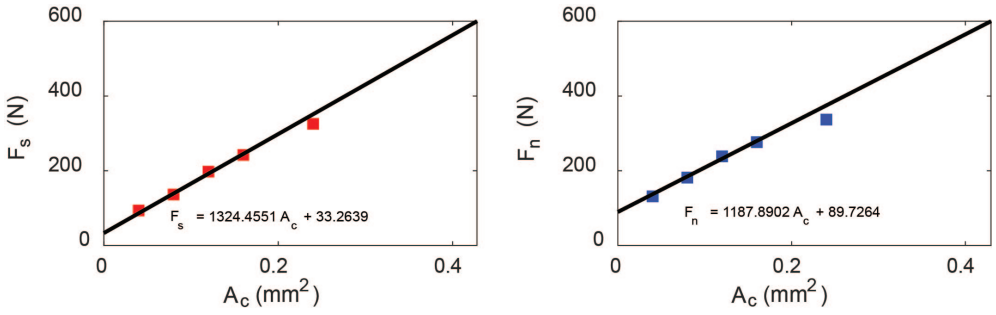

Figure A.3: The tangential force and normal force response of Crab orchard sandstone.

Donnybrook Sandstone

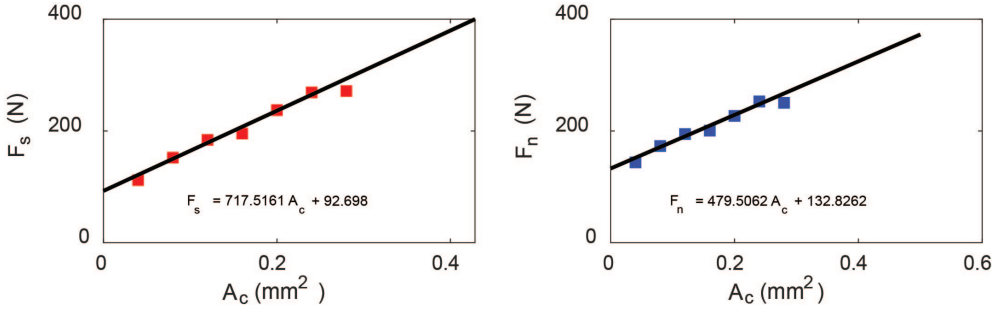

Figure A.4: The tangential force and normal force response of Donnybrook sandstone.

Grey Berea Sandstone

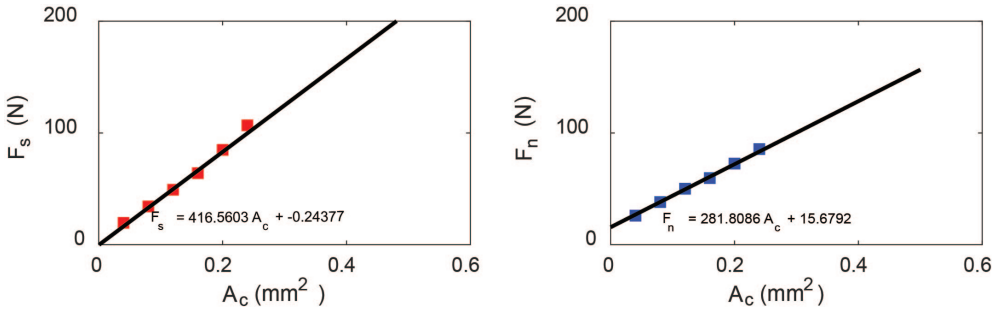

Figure A.5: The tangential force and normal force response of Grey Berea sandstone.

Indiana Limestone

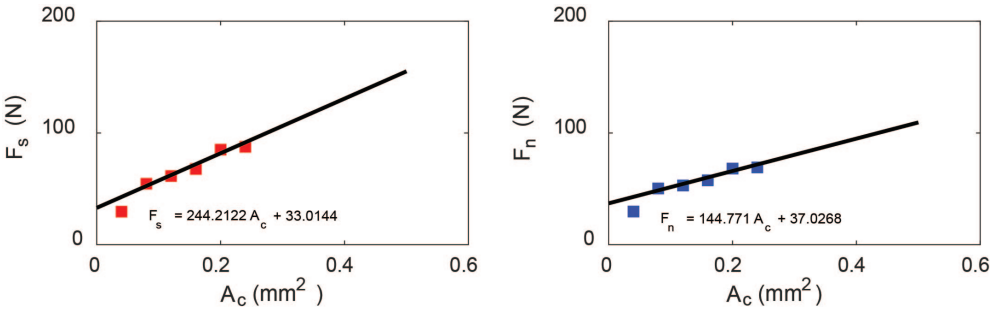

Figure A.6: The tangential force and normal force response of Indiana limestone.

Appendix B

UCS Standard Test

A sample is placed in a universal test machine and transducers are used to monitor the sample's axial and radial deformations as well as the axial load. Until the sample failed, it was axially loaded at a constant average axial displacement of 0.1797 mm/hour. The tangential slope of the curve of deviatoric stress versus average axial strain and the tangential slope of the curve of average radial strain versus average axial strain at between 40% and 60% of the maximum deviatoric stress are used to calculate the Young's modulus and Poisson's ratio.

Bluestone granite

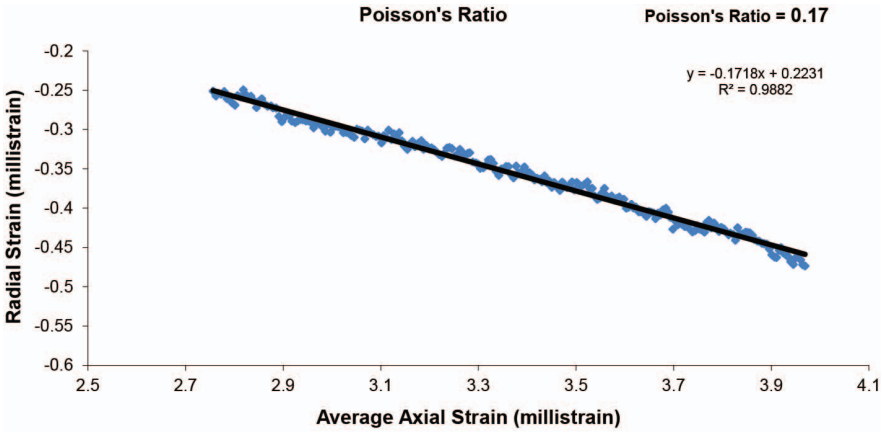

Figure B.1: Poisson's ratio measured from UCS standard test on Bluestone granite.

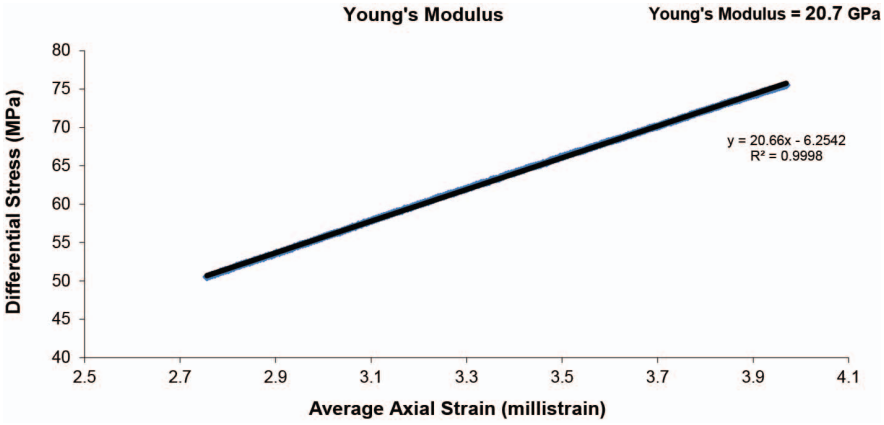

Figure B.2: Young's Modulus measured from UCS standard test on Bluestone granite.

Pre-Test Dry Density (g/cm^3) = 2.59

Unconfined Compressive strength (MPa)= 126.3

Calca red

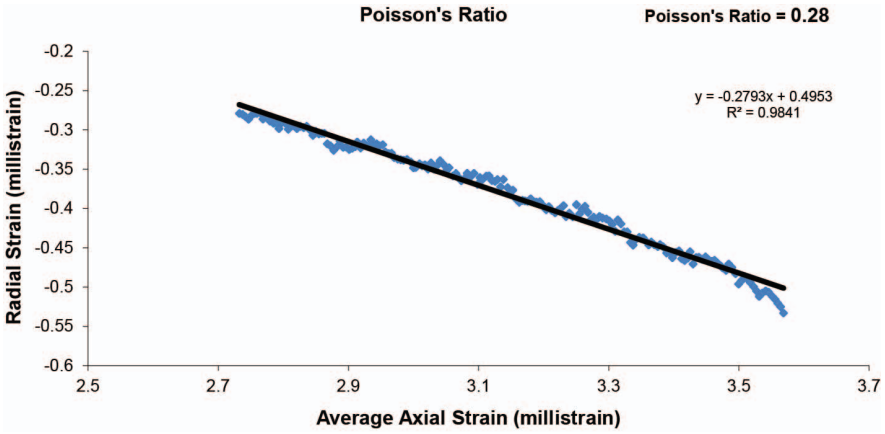

Figure B.3: Poisson's ratio measured from UCS standard test on Calca Red.

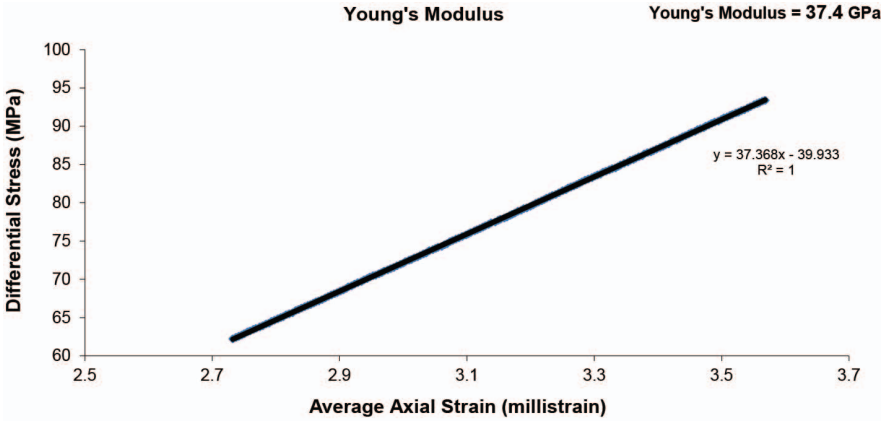

Figure B.4: Young's Modulus measured from UCS standard test on Calca Red.

Pre-Test Dry Density (g/cm^3) = 2.60

Unconfined Compressive strength (MPa)= 155.53

Guelph dolomite

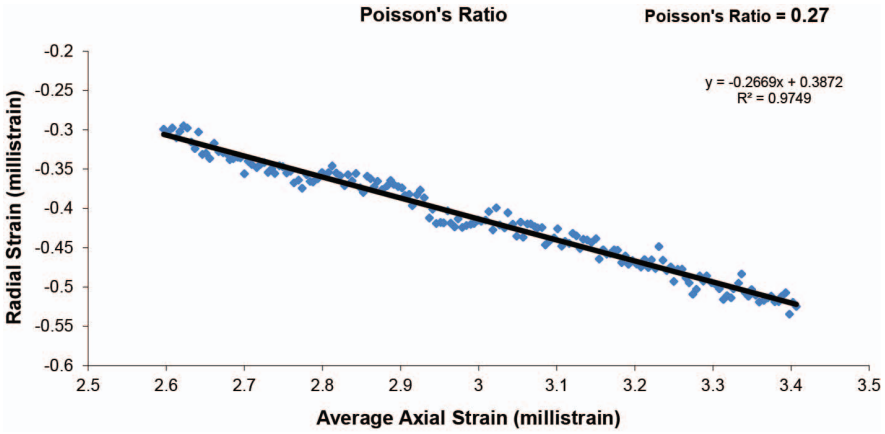

Figure B.5: Poisson's ratio measured from UCS standard test on Guelph dolomite.

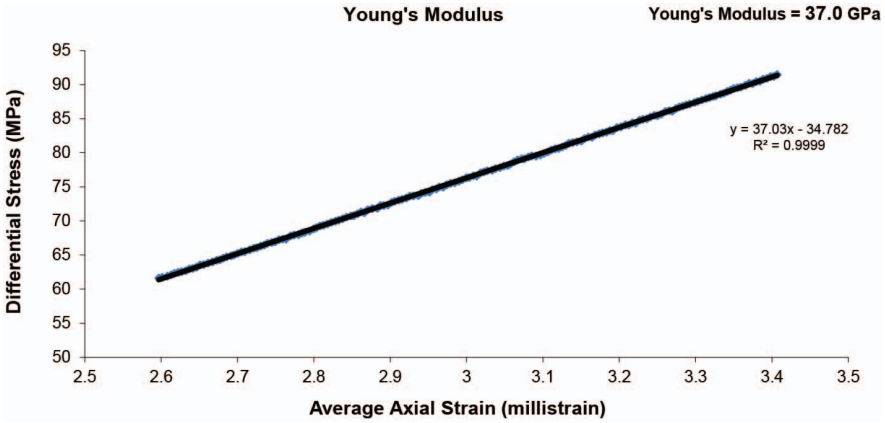

Figure B.6: Young's Modulus measured from UCS standard test on Guelph dolomite.

Pre-Test Dry Density (g/cm^3) = 2.64

Unconfined Compressive strength (MPa)= 151.6

Verde Austral

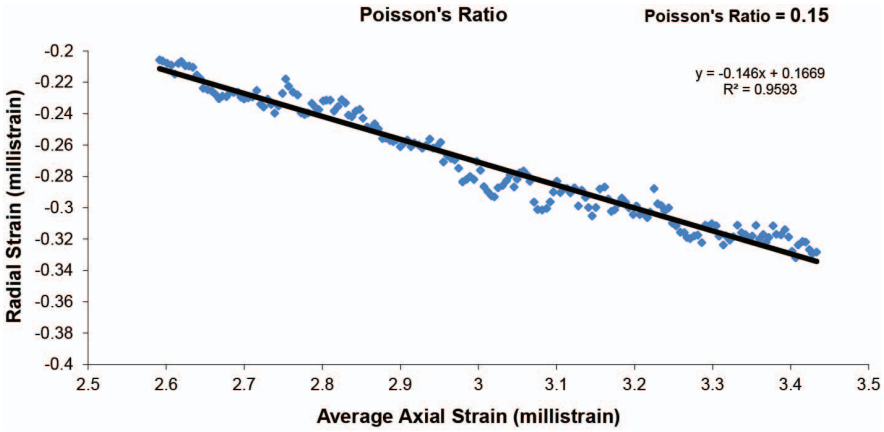

Figure B.7: Poisson's ratio measured from UCS standard test on Verde Austral.

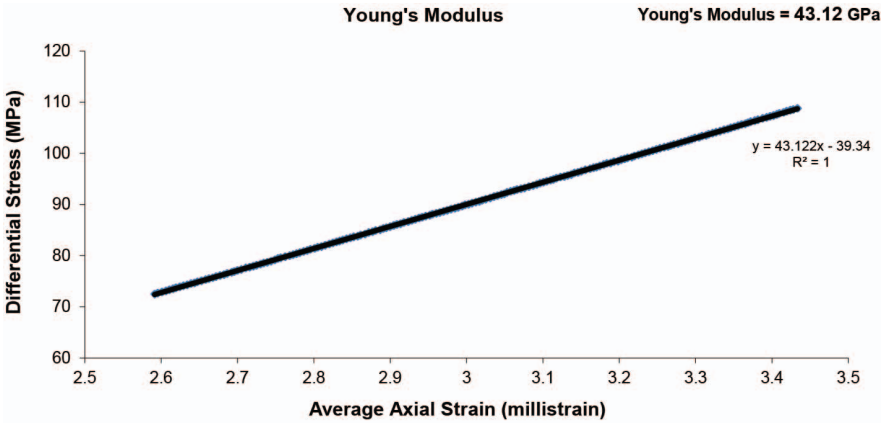

Figure B.8: Young's Modulus measured from UCS standard test on Verde Austral.

Pre-Test Dry Density (g/cm^3) = 2.63

Unconfined Compressive strength (MPa)= 181.3

Austral Black

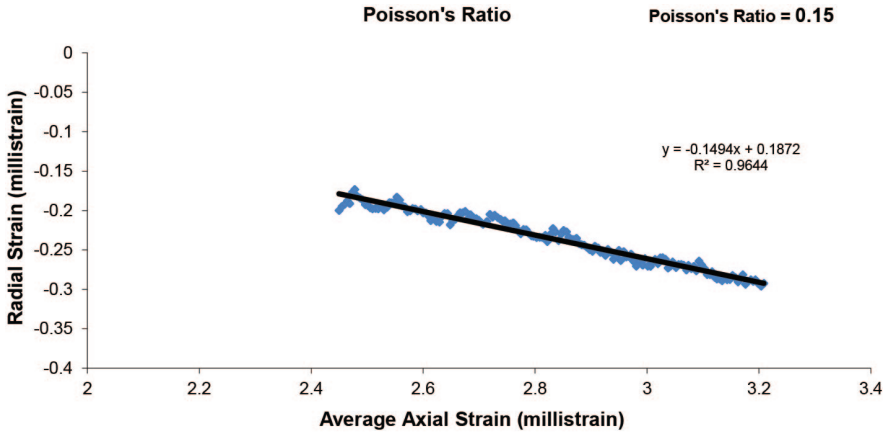

Figure B.9: Poisson's ratio measured from UCS standard test on Austral Black.

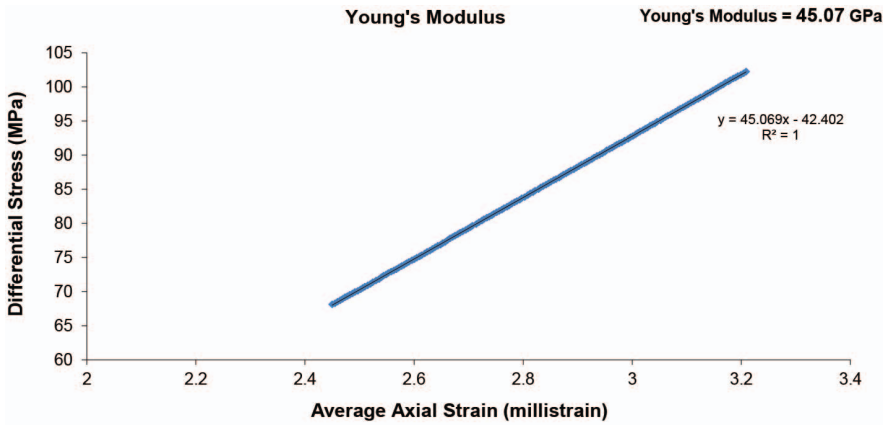

Figure B.10: Young's Modulus measured from UCS standard test on Austral Black.

Pre-Test Dry Density (g/cm^3) = 2.95

Unconfined Compressive strength (MPa)= 170.16

Appendix C

Two Body Abrasion Test

Two body abrasion test is a series of friction tests that measure coefficient of friction between tungsten carbide with respect to different rock samples using modified lathe cutting rig, Thor. The friction test uses a cylindrical matrix segment with no diamond cutters, by imposing a tiny amount of depth of cut, normal force and tangential force are measured. Coefficient of friction is evaluated by calculating the ratio of tangential to normal.

I derive the matrix-rock contact parameters (μ_m) from abrasion test carried out on Thor with a segment virgin of diamonds a very shallow depth of cut (5 $\mu m/rev$) while recording the normal and tangential component of the force acting on the segment, see Figure C.1. The friction of coefficient associated with matrix/rock contact is simply given

$$\mu_m = \frac{F_s}{F_n}$$

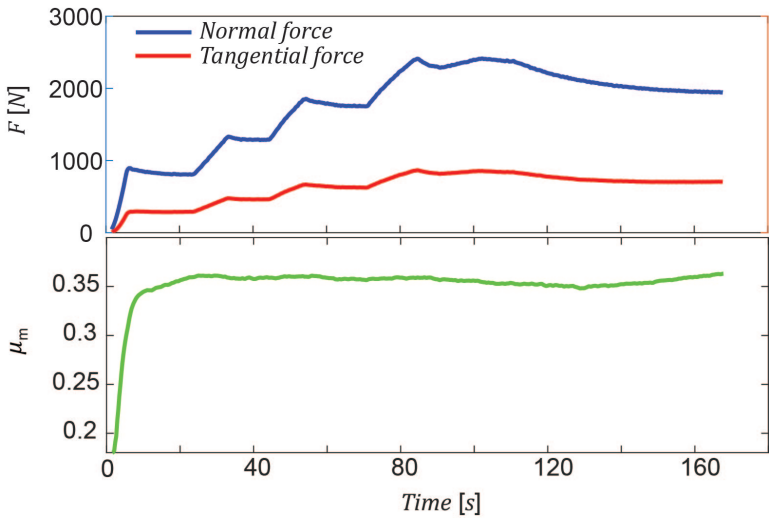

Figure C.1: Force responses of friction test on Austral Black using Thor.

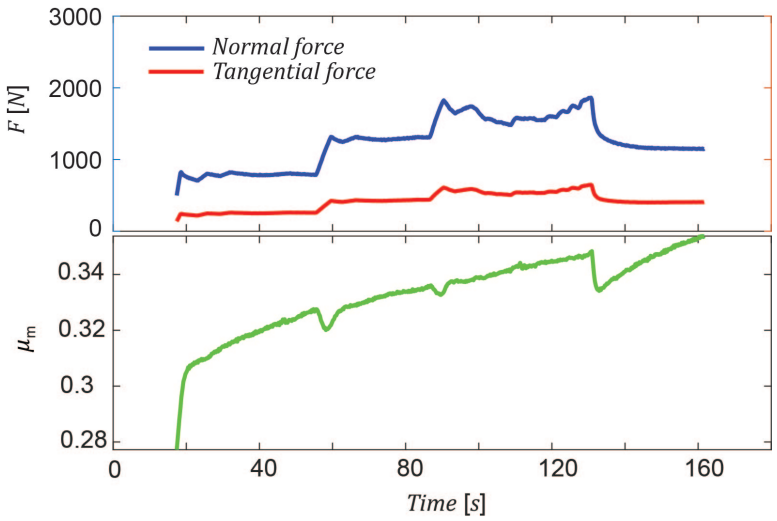

Figure C.2: Force responses of friction test on Bluestone granite using Thor.

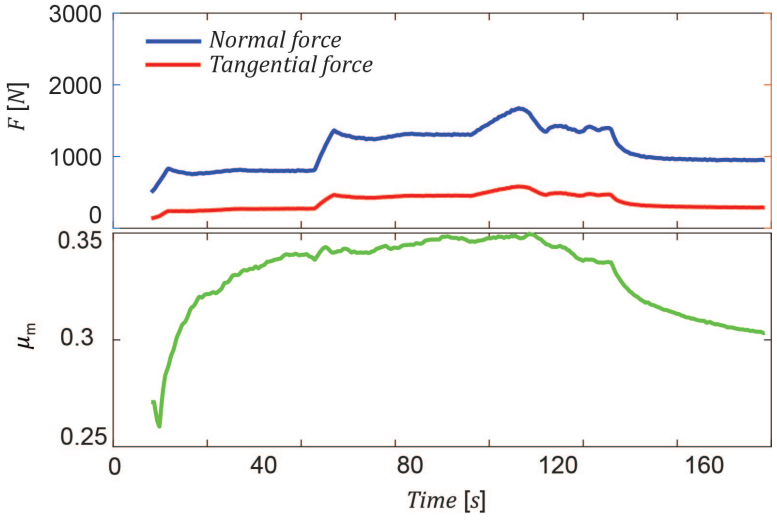

Figure C.3: Force responses of friction test on Calca red using Thor.

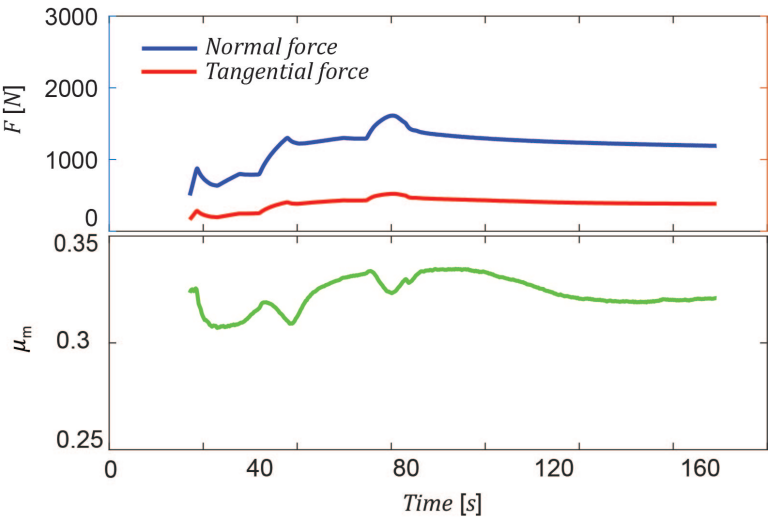

Figure C.4: Force responses of friction test on Colton sandstone using Thor.

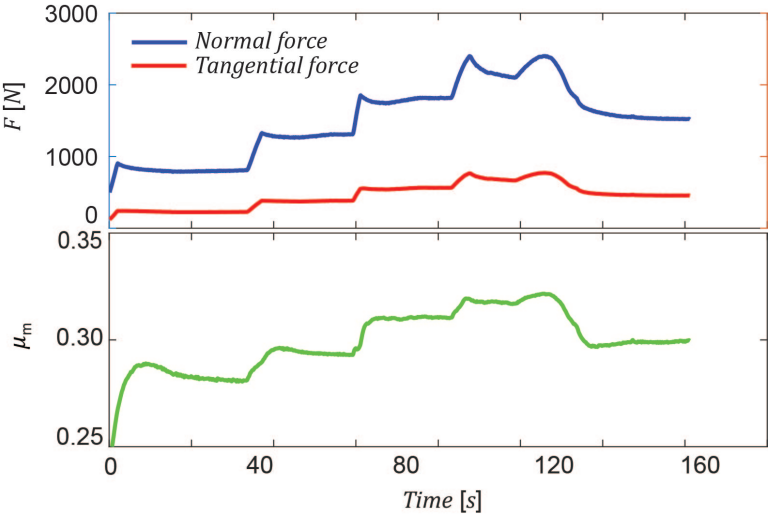

Figure C.5: Force responses of friction test on Donnybrook sandstone using Thor.

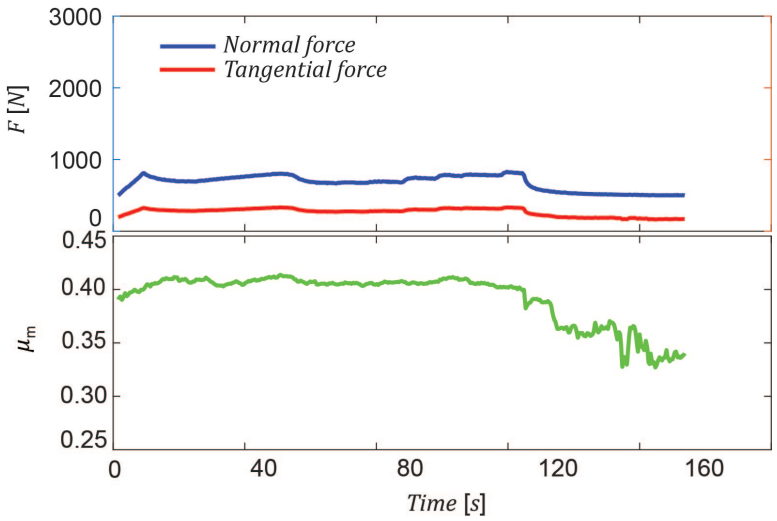

Figure C.6: Force responses of friction test on Guelph dolomite using Thor.

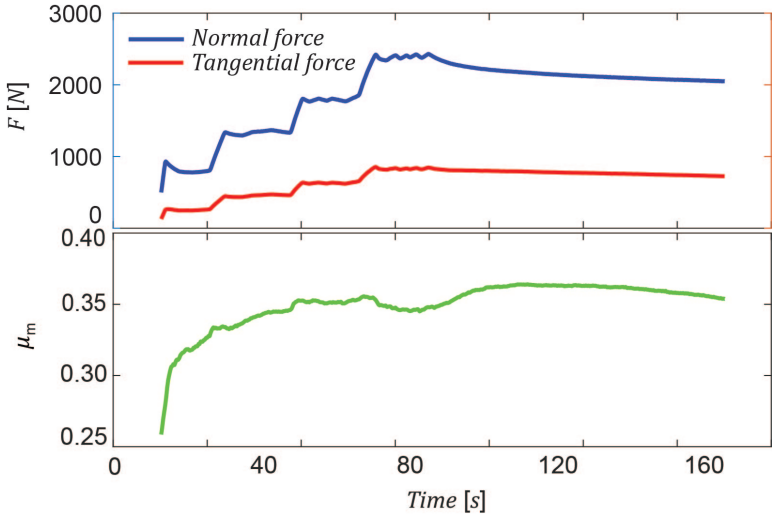

Figure C.7: Force responses of friction test on Verde austral using Thor.

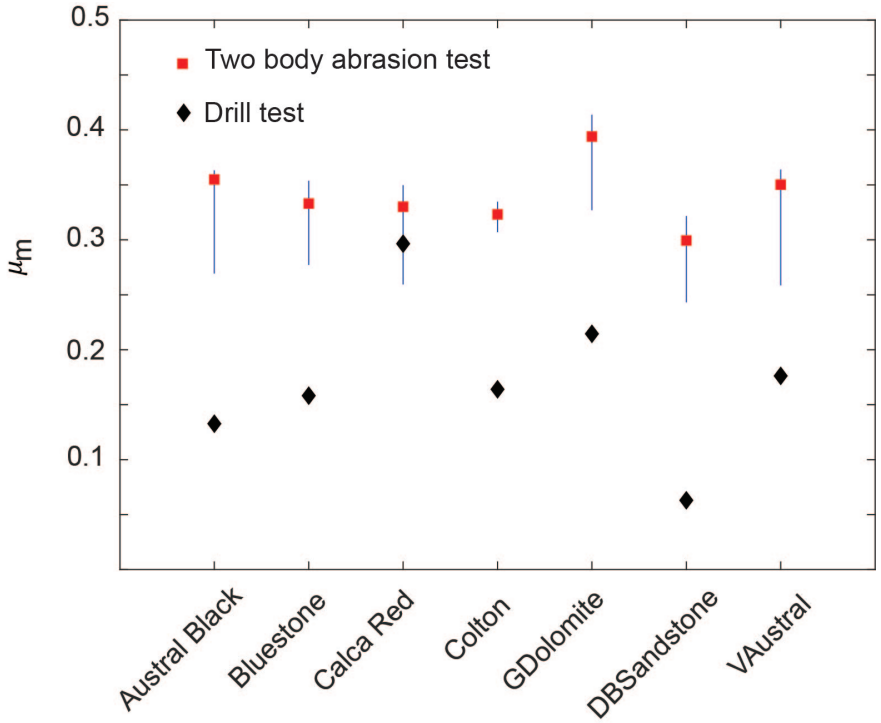

Figure C.8: Comparison of coefficient of friction measured in two body abrasion and three body abrasion.

Bibliography

B. Akbari, S. Miska, M. Yu, and R. Rahmani. The effects of size, chamfer geometry, and back rake angle on frictional response of pdc cutters. In *48th U.S. Rock Mechanics/Geomechanics Symposium*, volume All Days, ARMA-2014-7458, 2014.

G. R. Ballantyne, M. S. Powell, and M. Tiang. In *Proceedings of the 11th Australasian Institute of Mining and Metallurgy Mill Operator's Conference*, pages 25–30, 2012.

L. Battelle Memorial Institute. Columbus. *Final report on energy use patterns in metallurgical and nonmetallic mineral processing : to United States Bureau of Mines / Battelle Columbus Laboratories*. Columbus : The Laboratories, Columbus, 1975.

R. A. Bearman. Step change in the context of comminution. *Minerals Engineering*, 43-44:2–11, 2013. ISSN 0892-6875. doi: 10.1016/j.mineng.2012.06.010. URL https://dx.doi.org/10.1016/j.mineng.2012.06.010.

R. A. Bearman, C. A. Briggs, and T. Kojovic. The applications of rock mechanics parameters to the prediction of comminution behaviour. *Minerals Engineering*, 10(3):255–264, 1997. ISSN 0892-6875. doi: 10.1016/s0892-6875(97)00002-2. URL https://dx.doi.org/10.1016/s0892-6875(97)00002-2.

A. T. Bourgoyne and F. S. Young. A multiple regression approach to optimal drilling and abnormal pressure detection. *Society of Petroleum Engineers*

Journal, 14(04):371–384, 1974. ISSN 0197-7520. doi: 10.2118/4238-pa. URL https://dx.doi.org/10.2118/4238-pa.

J. B. Cheatham and W. H. Daniels. A study of factors influencing the drillability of shales: Single-cutter experiments with stratapax(t) drill blanks. *Journal of Energy Resources Technology*, 101(3):189–195, 1979. ISSN 0195-0738. doi: 10.1115/1.3446918. URL https://dx.doi.org/10.1115/1.3446918.

S. Chen, G. Grosz, S. Anderle, R. Arfele, and K. Xun. The role of rock-chip removals and cutting-area shapes in polycrystalline-diamond-compact-bit design optimization. *SPE Drilling Completion*, 30(04):334–347, 2016. ISSN 1064-6671. doi: 10.2118/171833-pa. URL https://dx.doi.org/10.2118/171833-pa.

F. Dagrain, E. Detournay, and T. Richard. Influence of cutter geometry in rock cutting. U.S. Rock Mechanics/Geomechanics Symposium, 07 2001. ARMA-01-0927.

E. Detournay and P. Defourny. A phenomenological model for the drilling action of drag bits. *International journal of rock mechanics and mining sciences geomechanics abstracts*, 29(1):13–23, 1992. ISSN 0148-9062. doi: 10.1016/0148-9062(92)91041-3.

E. Detournay, T. Richard, and M. Shepherd. Drilling response of drag bits: Theory and experiment. *International Journal of Rock Mechanics and Mining Sciences*, 45(8):1347–1360, 2008. ISSN 1365-1609. doi: https://doi.org/10.1016/j.ijrmms.2008.01.010. URL https://www.sciencedirect.com/science/article/pii/S1365160908000245.

S. Doshvarpassand, T. Richard, and M. Mostofi. Effect of groove geometry and cutting edge in rock cutting. *Journal of Petroleum Science and Engineering*, 151:1–12, 2017. ISSN 0920-4105. doi: https://doi.org/10.

1016/j.petrol.2017.01.023. URL https://www.sciencedirect.com/science/article/pii/S0920410516304314.

M. A. Elsayed and D. W. Raymond. Measurement and analysis of chatter in a compliant model of a drillstring equipped with a pdc bit. *No. SAND-99-2895C*, 11 1999. URL https://www.osti.gov/biblio/750032.

I. E. Eronini, W. H. Somerton, and D. M. Auslander. A Dynamic Model for Rotary Rock Drilling. *Journal of Energy Resources Technology*, 104(2):108–120, 06 1982. ISSN 0195-0738. doi: 10.1115/1.3230387. URL https://doi.org/10.1115/1.3230387.

L. F. P. Franca, M. Mostofi, and T. Richard. Interface laws for impregnated diamond tools for a given state of wear. *International Journal of Rock Mechanics and Mining Sciences*, 73:184–193, 2015. ISSN 1365-1609. doi: 10.1016/j.ijrmms.2014.09.010.

D. W. Fuerstenau and A. Z. M. Abouzeid. The energy efficiency of ball milling in comminution. *International Journal of Mineral Processing*, 67(1-4):161–185, 2002. ISSN 0301-7516. doi: 10.1016/s0301-7516(02)00039-x. URL https://dx.doi.org/10.1016/s0301-7516(02)00039-x.

L. Gerbaud, S. Menand, and H. Sellami. Pdc bits: All comes from the cutter/rock interaction. SPE, 2006. doi: 10.2118/98988-ms. URL https://dx.doi.org/10.2118/98988-ms.

D. Glowka. Design considerations for a hard rock pdc drill bit, 1985. URL https://www.osti.gov/biblio/5747583.

S. Gstalder and J. Raynal. Measurement of some mechanical properties of rocks and their relationship to rock drillability. *Journal of Petroleum Technology*, 18(08):991–996, 1966. ISSN 0149-2136. doi: 10.2118/1463-pa. URL https://dx.doi.org/10.2118/1463-pa.

G. W. Halsey, A. Kyllingstad, T. V. Aarrestad, and D. Lysne. Drillstring torsional vibrations: Comparison between theory and experiment on a full-scale research drilling rig. Society of Petroleum Engineers, 1986. doi: 10.2118/15564-ms. URL https://dx.doi.org/10.2118/15564-ms.

M. He, N. Li, J. Zhu, and Y. Chen. Advanced prediction for field strength parameters of rock using drilling operational data from impregnated diamond bit. *Journal of petroleum science engineering*, 187:106847, 2020. ISSN 0920-4105. doi: 10.1016/j.petrol.2019.106847.

S. Huband, L. Barone, P. Hingston, L. While, D. Tuppurainen, and R. Bearman. Designing comminution circuits with a multi-objective evolutionary algorithm. volume 2, pages 1815–1822 Vol. 2, 2005. doi: 10.1109/CEC.2005.1554908.

S. Kahraman, N. Bilgin, and C. Feridunoglu. Dominant rock properties affecting the penetration rate of percussive drills. *International Journal of Rock Mechanics and Mining Sciences*, 40(5):711–723, 2003. ISSN 1365-1609. doi: https://doi.org/10.1016/S1365-1609(03)00063-7. URL https://www.sciencedirect.com/science/article/pii/S1365160903000637.

L. A. Kennedy and J. G. Spray. Frictional melting of sedimentary rock during high-speed diamond drilling: an analytical sem and tem investigation. *Tectonophysics*, 204(3):323–337, 1992. ISSN 0040-1951. doi: https://doi.org/10.1016/0040-1951(92)90315-W. URL https://www.sciencedirect.com/science/article/pii/004019519290315W.

G. C. Lowrison. *Crushing and grinding : the size reduction of solid materials*. CRC Press, London, 1974. ISBN 0878190627.

W. Maurer. Bit-tooth penetration under simulated borehole conditions, the state of rock mechanics knowledge in drilling. In *The 8th U.S. Symposium on Rock Mechanics (USRMS)*, volume All Days, ARMA-66-0355, 1966.

F. McFeat, Smith; R.J. Correlation of rock properties and the cutting performance of tunnelling machines. *International Journal of Rock Mechanics and Mining Sciences Geomechanics Abstracts*, 14(5-6):A87, 1977. ISSN 0148-9062. doi: 10.1016/0148-9062(77)90837-3. URL https://dx.doi.org/10.1016/0148-9062(77)90837-3.

M. Mellor. Normalization of specific energy values. *International Journal of Rock Mechanics and Mining Sciences Geomechanics Abstracts*, 9(5):661–663, 1972. ISSN 0148-9062. doi: 10.1016/0148-9062(72)90016-2. URL https://dx.doi.org/10.1016/0148-9062(72)90016-2.

M. Mostofi. *Drilling response of impregnated diamond bits: modelling and experimental investigations*. Thesis, Curtin University, Department of Petroleum Engineering, 2014.

M. Mostofi, V. Rasouli, and E. Mawuli. An estimation of rock strength using a drilling performance model: A case study in blacktip field, australia. *Rock Mechanics and Rock Engineering*, 44(3):305, 2011. ISSN 1434-453X. doi: 10.1007/s00603-011-0142-9. URL https://doi.org/10.1007/s00603-011-0142-9.

A. S. Murray and R. A. Cunningham. Effect of mud column pressure on drilling rates. *Transactions of the AIME*, 204(01):196–204, 1955. ISSN 0081-1696. doi: 10.2118/505-g. URL https://dx.doi.org/10.2118/505-g.

A. Mwanga, J. Rosenkranz, and P. Lamberg. Testing of ore comminution behavior in the geometallurgical context—a review. *Minerals*, 5(2):276–297, 2015. ISSN 2075-163X. URL https://www.mdpi.com/2075-163X/5/2/276.

T. Napier-Munn, D. Drinkwater, and G. Ballantyne. The ceec roadmap for eco-efficient comminution. page 15, June 2012.

J. Paone, W. E. Bruce, and P. R. Virciglio. *Drillability studies: statistical regression analysis of diamond drilling*. US Department of the Interior, Bureau of Mines, 1966a.

J. Paone, P. R. Virciglio, W. E. Bruce, and S. United. *Drillability studies: statistical regression analysis of diamond drilling.* Report of investigations / United States Department of the Interior, Bureau of Mines ;6880. U.S. Dept. of the Interior, Bureau of Mines, [Washington, D.C.], 1966b. URL //catalog.hathitrust.org/Record/005951838http://hdl.handle.net/2027/mdp.39015078511246.

J. L. Peterson. Diamond drilling model verified in field and laboratory tests. *Journal of Petroleum Technology*, 28(02):213–222, 1976. ISSN 0149-2136. doi: 10.2118/5072-pa. URL https://dx.doi.org/10.2118/5072-pa.

H. Rabia. Specific energy as a criterion for drill performance prediction. *International Journal of Rock Mechanics and Mining Sciences Geomechanics Abstracts*, 19(1):39–42, 1982. ISSN 0148-9062. doi: 10.1016/0148-9062(82)90709-4. URL https://dx.doi.org/10.1016/0148-9062(82)90709-4.

T. Richard, E. Detournay, A. Drescher, P. Nicodeme, and D. Fourmaintraux. The scratch test as a means to measure strength of sedimentary rocks. SPE, 1998. doi: 10.2118/47196-ms. URL https://dx.doi.org/10.2118/47196-ms.

T. Richard, F. Dagrain, E. Poyol, and E. Detournay. Rock strength determination from scratch tests. *Engineering geology*, 147-148:91–100, 2012. ISSN 0013-7952. doi: 10.1016/j.enggeo.2012.07.011.

M. M. Sharma and R. W. Wunderlich. The alteration of rock properties due to interactions with drilling-fluid components. *Journal of Petroleum Science and Engineering*, 1(2):127–143, 1987. ISSN 0920-4105. doi: 10.1016/0920-4105(87)90004-0. URL https://dx.doi.org/10.1016/0920-4105(87)90004-0.

L. A. Sinor and T. M. Warren. Drag bit wear model. SPE, 1987. doi: 10.2118/16699-ms. URL https://dx.doi.org/10.2118/16699-ms.

R. Teale. The concept of specific energy in rock drilling. *International Journal of Rock Mechanics and Mining Sciences Geomechanics Abstracts*, 2(1):57–

73, 1965. ISSN 0148-9062. doi: 10.1016/0148-9062(65)90022-7. URL https://dx.doi.org/10.1016/0148-9062(65)90022-7.

K. Thuro. Drillability prediction: geological influences in hard rock drill and blast tunnelling. *Geologische Rundschau*, 86(2):426–438, 1997. ISSN 1432-1149. doi: 10.1007/s005310050151. URL https://doi.org/10.1007/s005310050151.

B. Tiryaki and A. C. Dikmen. Effects of rock properties on specific cutting energy in linear cutting of sandstones by picks. *Rock Mechanics and Rock Engineering*, 39(2):89–120, 2006. ISSN 1434-453X. doi: 10.1007/s00603-005-0062-7. URL https://doi.org/10.1007/s00603-005-0062-7.

T. M. Warren. Penetration rate performance of roller cone bits. *SPE drilling engineering*, 2(1):9–18, 1987. ISSN 0885-9744. doi: 10.2118/13259-PA.

W. J. Winters, T. M. Warren, and E. C. Onyia. Roller bit model with rock ductility and cone offset. SPE, 1987. doi: 10.2118/16696-ms. URL https://dx.doi.org/10.2118/16696-ms.

E. Yaşar, P. G. Ranjith, and D. R. Viete. An experimental investigation into the drilling and physico-mechanical properties of a rock-like brittle material. *Journal of Petroleum Science and Engineering*, 76(3):185–193, 2011. ISSN 0920-4105. doi: https://doi.org/10.1016/j.petrol.2011.01.011. URL https://www.sciencedirect.com/science/article/pii/S0920410511000222.

M. B. Ziaja and S. Miska. Mathematical model of the diamond-bit drilling process and its practical application. *Society of Petroleum Engineers Journal*, 22(06): 911–922, 1982. ISSN 0197-7520. doi: 10.2118/10148-pa. URL https://dx.doi.org/10.2118/10148-pa.

D. H. Zijsling. Single cutter testing - a key for pdc bit development. SPE, 1987. doi: 10.2118/16529-ms. URL https://dx.doi.org/10.2118/16529-ms.

W. A. Zoeller. Analysis of rock properties from drilling response. SPWLA Annual Logging Symposium, June 1974. SPWLA-1974-N.